

8-2017

BASIGIN-2 MEDIATED ACTIVATION OF ERK1/2 SIGNALING IN HUMAN GLIOBLASTOMA MULTIFORME CELLS

Erik R. Peterson
Northern Michigan University, eripeter@nmu.edu

Follow this and additional works at: <https://commons.nmu.edu/theses>



Part of the [Biology Commons](#), [Cancer Biology Commons](#), and the [Cell Biology Commons](#)

Recommended Citation

Peterson, Erik R., "BASIGIN-2 MEDIATED ACTIVATION OF ERK1/2 SIGNALING IN HUMAN GLIOBLASTOMA MULTIFORME CELLS" (2017). *All NMU Master's Theses*. 159.
<https://commons.nmu.edu/theses/159>

This Open Access is brought to you for free and open access by the Student Works at NMU Commons. It has been accepted for inclusion in All NMU Master's Theses by an authorized administrator of NMU Commons. For more information, please contact kmcdonou@nmu.edu, bsarjean@nmu.edu.

BASIGIN-2-MEDIATED ACTIVATION OF ERK1/2 SIGNALING IN HUMAN
GLIOBLASTOMA MULTIFORME CELLS

By

Erik Peterson

THESIS

Submitted to
Northern Michigan University
In partial fulfillment of the requirements
For the degree of

MASTER OF SCIENCE

Office of Graduate Education and Research

June 26th, 2017

SIGNATURE APPROVAL FORM

Basigin-2 mediated activation of ERK1/2 signaling in human Glioblastoma Multiforme cells

This thesis by Erik Peterson is recommended for approval by the student's Thesis Committee and Department Head in the Department of Biology and by the Assistant Provost of Graduate Education and Research.

Committee Chair: Date

First Reader: Date

Second Reader (if required): Date

Department Head: Date

Dr. Lisa S. Eckert Date
Interim Director of Graduate Education

ABSTRACT

BASIGIN-2 MEDIATED ACTIVATION OF ERK1/2 SIGNALING IN HUMAN GLIOBLASTOMA MULTIFORME CELLS

By

Erik Peterson

Glioblastoma multiforme (GBM) is the most common malignant form of human brain cancer. GBM tumor cells overexpress the protein Basigin (Bsg) at the cell surface where it contributes to malignancy via stimulation of matrix metalloproteinase (MMP) expression in surrounding normal tissues, resulting in the degradation of the extracellular matrix (ECM) surrounding tumors, promoting remodeling of the tumor borders, stimulating growth. In work by Belton et al. (2008), human uterine endometrial cells treated with a recombinant form of human basigin possessing the extracellular domain of the Bsg protein (rBsg-ECD) showed activation of the Mitogen-Activated Protein Kinase (MAPK) signaling pathway proteins, ERK1/2. This effect was mediated by rBsg-ECD binding to the Basigin-2 (Bsg-2) at the cell surface. In this research, U87-MG human GBM cells were treated with purified rBsg-ECD protein to measure changes in the phosphorylation of the ERK1/2 proteins. The results indicate the presence of a signaling loop within GBM tumors where soluble Bsg protein stimulates signal transduction through Bsg-2 at the cell surface. rBsg-mediated ERK1/2 stimulation is inhibited by the antioxidant compound Resveratrol, suggesting that the signaling mechanism through Bsg-2 involves the Epidermal Growth Factor Receptor (EGFR). Taken together, these results indicate that soluble Basigin protein stimulates signaling events through the MAPK signaling pathway by binding to Bsg-2 on the surface of GBM cells.

Copyright by

Erik Peterson

June, 2017

ACKNOWLEDGMENTS

The completion of this thesis would not have been possible if not for the support of the Upper Michigan Brain Tumor Center, Excellence in Education Grant, and graduate and tutorial assistantships. I would like to thank my committee members Dr. Robert Belton, Dr. John Lawrence, Dr. John Rebers, and Dr. Josh Sharp for their guidance and support of my research. I would also like to thank Marissa Kane, Nick Shortreed, Aaron Mellesmoen, Amanda Wigand, and Samantha Wightman for their assistance and advice. Finally, I must recognize Gregory and Kathleen Peterson for their support and encouragement of my goal throughout my life and collegiate career.

TABLE OF CONTENTS

Introduction.....	1
Aims and Goals.....	18
Methods and Materials.....	20
Cell Culture.....	20
Control and Experimental Protein Lysate Collection.....	20
Bacterial Cell Culture.....	22
rBsg Isolation.....	22
rBsg Treatment of U87-MG Cells and Protein Lysate Collection.....	25
Sulfo-SBED rBsg Binding Assay.....	25
Western Blot Analysis.....	27
Results.....	30
Recombinant Basigin Isolation, Purification, and Analysis.....	30
Early Control Cell Lysate Collection Attempts.....	32
Antibody Nonspecific Binding Test Assay.....	34
Resveratrol Treatment Assay.....	34
Unstimulated Baseline ERK1/2 Phosphorylation in U87-MG Cells.....	36
Serum-Stimulated ERK1/2 Phosphorylation in U87-MG Cells.....	37
rBsg Treatment of U87-MG Cells.....	38
Sulfo-SBED Label Transfer Assay.....	40
Discussion.....	66

Conclusion.....	76
Works Cited.....	77
Appendices.....	82
License to use Figure 2 from “Integration of EGFR inhibitors with radiochemotherapy” by Nyati et al. received from Nature Publishing Group.....	82
License to use Figures 1 and 2 from “The microenvironment of the tumour-host interface” by Liotta and Kohn received from Nature Publishing Group.....	83

LIST OF FIGURES

Figure 1: The EGFR receptor transduces signals along multiple signaling pathways.....	15
Figure 2: Mechanism for tumor cell invasion.....	16
Figure 3: Molecular communication at the tumor invasion front.....	17
Figure 4: SDS-PAGE analysis of rBsg-ECD elution fractions.....	43
Figure 5: SDS-PAGE of concentrated rBsg-ECD and unbound protein fractions.....	44
Figure 6: SDS-PAGE of final rBsg-ECD purification.....	45
Figure 7: Coomassie blue stained SDS-PAGE of serial diluted rBsg-ECD.....	46
Figure 8: Basigin immunoblot analysis of rBsg-ECD dilution series.....	47
Figure 9: Analysis of ERK1/2 expression in U87MG cells treated with FBS.....	48
Figure 10: Analysis of ERK1/2 activation in U87MG cells treated with FBS.....	49
Figure 11: Repeat analysis of ERK1/2 activation in U87MG cells treated with FBS.....	50
Figure 12: Repeat analysis of ERK1/2 expression in U87MG cells treated with serum-free media.....	51
Figure 13: Jurkat T-cell lysate immunoblots for phosphorylated ERK1/2.....	52
Figure 14: Primary and secondary antibody control immunoblot analysis.....	53

Figure 15: Characterization of the effects of Resveratrol on ERK1/2 activation in U87MG cells treated with FBS.....	54
Figure 16: Pre-treatment and Co-treatment of cells with 30µM RSV produces the greatest amount of inhibition of FBS-stimulated ERK1/2 activation in U87MG cells.....	55
Figure 17: RSV treatment of U87MG cells to determine baseline ERK1/2 expression and phosphorylation levels.....	56
Figure 18: Resveratrol treatment of U87MG cells reduces FBS-induced ERK1/2 phosphorylation at room temperature (21°C).....	57
Figure 19: Resveratrol treatment of U87MG cells reduces FBS-induced ERK1/2 phosphorylation at body temperature (37°C).....	58
Figure 20: Resveratrol treatment of U87MG cells reduces peak FBS-induced ERK1/2 phosphorylation at body temperature (37°C).....	59
Figure 21: Initial immunoblot analysis of U87MG cells treated with rBsg or rBsg+30µM RSV.....	60
Figure 22: Revised immunoblot analysis of U87MG cells treated with rBsg or rBsg+30µM RSV.....	61
Figure 23: Resveratrol treatment of U87MG cells reduces peak rBsg-induced ERK1/2 phosphorylation at body temperature (37°C).....	62
Figure 24: NeutrAvidin-HRP Blot for Putative Receptors of rBsg-SBED Bait Protein...	63
Figure 25: Evidence for rBsg-ECD labeling of U87MG cells and the activation of the ERK1/2 signaling pathway.....	64
Figure 26: Second Attempt of NeutrAvidin-HRP Blots for Putative Receptors of rBsg-SBED Bait Protein.....	65

LIST OF ABBREVIATIONS

GBM-	Glioblastoma Multiforme
Bsg-	Basigin
MMP-	Matrix Metalloproteinase
ECM-	Extracellular Matrix
MAPK-	Mitogen Activated Protein Kinase
rBsg-	Recombinant Basigin
rBsg-ECD-	Recombinant Basigin Extracellular Domain
Bsg-2-	Basigin-2
ERK1/2-	Extracellular Signal-Regulated Kinases 1 and 2
pERK1/2	Phosphorylated (Phospho-) ERK1/2
EGFR-	Epidermal Growth Factor Receptor
EGFRvIII-	Epidermal Growth Factor Receptor Variant III
kDa-	kiloDalton
Ig-	Immunoglobulin
TCSF-	Tumor Collagenase Stimulating Factor
RNA-	Ribonucleic Acid
VEGF-	Vascular Endothelial Growth Factor
MVD-	Mevalonate Diphosphate Decarboxylase
ATP-	Adenosine-5'-Triphosphate
MCT-	Monocarboxylate Transporter
Cyp-	Cyclophilin
RSV-	Resveratrol
TMZ-	Temozolomide
DNA-	Deoxyribonucleic Acid

MGMT-	O'6-Methylguanine DNA-Methyltransferase
FBS-	Fetal Bovine Serum
BCA-	Bicinchoninic Acid Assay
Amp-	Ampicillin
Chl-	Chloramphenicol
OSL-	Osmotic Shock Lysate

INTRODUCTION

Glioblastoma multiforme (GBM), or Grade IV astrocytoma, is the most common malignant form of human brain cancer, representing 15% of all brain tumors diagnosed in patients². These tumors are generally located in the cerebral white matter of the brain and generally arise from a population of glial cells called astrocytes. GBM tumors characteristically possess a central core of necrotic (dying) tissue surrounded by anaplastic (rapidly growing) cells that exhibit limited differentiation characteristics. The outer border of the tumor generally possesses a high degree of vascularized tissue which is thought to develop in response to the resulting low oxygen levels within the tumor microenvironment. Prognosis for patients that develop of a GBM tumor is very grim. The general life expectancy following diagnosis is 12 to 15 months with a five-year survival rate to 3-5%³. The current standard of care is to aggressively resect the tumor and provide local radiation therapy, as well as chemotherapy using the prodrug temozolomide. Unfortunately, many patients experience the recurrence of tumors that are resistant to temozolomide following treatment⁴. Recurrence of the tumor, even after maximum treatment, is common and most likely attributed to a population of tumor-initiating cancer stem cells that resist most known conventional treatment methods.

The aggressive nature of the disease can be attributed to changes in the molecular biology of the tumor cells. For example, the epidermal growth factor receptor gene

(*EGFR*) is one of the most commonly mutated genes in GBM tumors, and changes to the EGFR gene and protein, or the signaling cascade emanating from it promote pro-survival signaling cascades leading to tumor growth⁵. Often times, GBM tumors will express a variant of the EGFR called EGFRvIII, consisting of a truncated and constitutively active form of the EGFR protein⁶. Constitutively activated EGFR vIII activates the Mitogen Activated Protein Kinase (MAPK) signaling pathway in the absence of normal ligand-receptor interactions leading to changes in gene expression within the tumor. The EGFR signaling pathway possesses a number of other signaling molecules that when mutated can also potently induce a pro-cancerous phenotype. This includes the enzymes Raf, MEK, and ERK1/2, which all function together with EGFR and the small G-protein Ras to promote stimulation of the cell cycle resulting in the inappropriate growth of cells. Understanding how all of these proteins work together to promote the progression of GBM tumors is crucial to the development of new and more effective treatments.

In the tumor microenvironment, one of the main factors driving tissue remodeling and promoting metastasis and tumor cell growth is the protein Basigin-2 (Bsg-2). This immunoglobulin-like transmembrane glycoprotein is known by several other names, including EMMPRIN and CD147, and is commonly expressed in human endothelial cells and red blood cells, with known roles in tissue remodeling required for mammalian embryonic implantation and development of retinal cells in the eye^{1, 8}. Basigin is also implicated in spermatogenesis, fertilization, and lymphocyte responsiveness, due to its wide expression across numerous lymphatic cells⁹. There are currently four known isoforms of the basigin protein, Bsg-1-4, but the functions of Bsg-1, -3, and -4 are not well understood¹. The Bsg-2 protein possesses two Ig-like loops, each stabilized by

disulfide bridges between cysteine residues at amino acids 157 and 203 and the 242 and 301, respectively, in the Bsg-2 sequence. All Basigin isoforms also possess a conserved transmembrane sequence and a short cytoplasmic domain that possesses no known signaling domain.

The predominant form of human basigin found in cells (Bsg-2) possesses 269 amino acids with a core mass of 29.2 kDa ([UNIPROT Entry P35613](#))⁹. Bsg-2 can be glycosylated on three asparagine residues as it transits through the secretory pathway resulting in two forms of the molecule containing variable amounts of glycosylation: the high-glycosylated form has a mass of 50-60 kDa and a low-glycosylated form has a mass of approximately 42kDa.^{10, 11} Basigin-2 possesses high-mannose and complex-type glycan structures attached to three asparagine sites in the high glycosylated form (at amino acids 160, 278, and 302), and one polysaccharide group attached to the asparagine at position 302 in the low glycosylated form¹¹⁻¹³. The degree of glycosylation appears to control subcellular localization and protein interactions. The low glycosylated form interacts preferentially with the protein caveolin-1, which appears to prevent the complex from interacting with other factors within the cell and is prevented from forming clusters^{10, 12}. When the protein is highly glycosylated, Bsg-2 can form aggregates at the cell surface, where it possesses biological activity by stimulating surrounding cells through direct cell-cell interactions or through release of membrane vesicles containing Bsg-2. Furthermore, the high glycosylated form of Bsg-2 is known to associate with additional membrane proteins such as integrin $\alpha 3\beta 1$ to promote cellular migration through the ECM and internal cellular architectural alterations¹⁴.

One of the hallmarks of any cancer is its ability to spread from its primary growth site to secondary locations in a process called metastasis. There are multiple barriers to metastasis, including the physical barrier of the basement membrane proteins of the extracellular matrix (ECM). In order for cancer cells to spread into surrounding tissues, they must break down this physical barrier produced and secreted by normal mesenchymal cells such as stromal fibroblasts. Such fibroblast cells also possess the ability to produce the enzymes required to remodel the ECM as needed. This is accomplished through the production of a family of enzymes called matrix-metalloproteinases (MMPs). Interestingly, elevated expression of Bsg-2 in cancer cells can induce surrounding fibroblasts to express MMPs that function to degrade the ECM, facilitating break down of the basement membrane separating tissues to promote tumor metastasis^{1, 14-18}. In fact, it was this observation that led to Bsg-2 previously being named the Extracellular Matrix MetalloPRoteinase Inducer¹⁹. Early studies by Chitra Biswas (1984) suggested that a soluble factor released from carcinoma cells called Tumor cell-derived Collagenase Stimulating Factor (TCSF) was able to stimulate normal fibroblasts to produce the MMPs 1-3²⁰. Subsequently, TCSF was shown to be a soluble form of the Bsg-2 protein²⁰.

In tumor tissue, particularly GBM tissue, Bsg is usually overexpressed on the cell surface within lipid rafts²¹⁻²³. During the process of vesicular shedding, budding pieces of tumor cell membrane containing high levels of Bsg-2 are released into the ECM, targeting stromal fibroblasts, other tumor cells, or other healthy cell types found in the local area of the tumor. The binding of Bsg-2 at the cellular surface has been shown to induce MMP expression in stromal fibroblasts, causing degradation of the ECM¹⁴⁻¹⁸. Bsg

stimulates the release of various MMPs, most notably MMPs-2, and -9 in GBMs. Through the use of antisense RNA to block Bsg function, MMP-2/-9 secretions in GBM cells were decreased heavily, along with vascular endothelial growth factor (VEGF)²⁴. In other work performed by Sameshima et al. (2000), Bsg was found to induce MMP expression in brain-derived fibroblast cells, implicating this complex relationship in the human brain²⁷. This work also illustrated the ability of Bsg-2 to stimulate the production of activated Gelatinase A (MMP-2) which cleaves both gelatinous and collagenous filaments in the ECM, via the increased production of “membrane type” MMPs-1 and -2. Through the inhibition of Bsg-2 with function-blocking antibody, secreted levels of both “membrane type” MMPs and MMP-2 were decreased²⁴.

In healthy tissue, MMP production and subsequent enzymatic action is implemented in tissue remodeling and repair after damage or in response to cell growth. However, in cancer, with the matrix degraded, dividing tumor cells can move into the space, causing growth of the tumor. As this process continues, cancerous cells are able to continuously gain ground within the body, eventually reaching vascular tissue, which it can use as an expressway to another location in the body to establish a site of metastasis. In conjunction with MMP induction and extracellular matrix degradation, Bsg-2 can associate with proteins known as integrins, which possess two different subunits, alpha (α) and beta (β), that determine their exact function depending on the combination of alpha and beta subunits. These proteins function mechanically to move a cell through the ECM by facilitating and sensing adhesion to the ECM. When normal cells don't receive a signal through their integrins at their surfaces, they can be subjected to the process of anoikis where the cell will undergo apoptosis due to detachment to the ECM²⁵. This

biological mechanism is designed to prevent the detachment and relocation of cells to new tissues. Cancerous cells are able to avoid anoikis and spread, believed to be partially mediated by the interaction between basigin and integrins. Cells overexpressing the basigin-2 protein have been shown to be able to grow and proliferate independent of basement membrane attachment in a *Drosophila melanogaster* model²⁵. Bsg-2 association with integrin $\alpha 6\beta 1$, particularly the overexpression of both, is known to increase the invasiveness of hepatoma tumor cells, evidenced by the decrease in invasive potential when knocked down with function blocking antibodies against $\alpha 6\beta 1$ ²⁶. Bsg-2/ $\alpha 3\beta 1$ interaction produces similar effects, as well upregulation of proteins downstream of integrins in their signaling pathway²⁸. In the context of GBM cells, not much research has found a relationship between basigin and integrin expression and action. However, there is evidence that integrin $\alpha 6$, which associates with Bsg-2, is involved in the regulation of GBM stem cells and serves as a glioblastoma stem cell marker²⁷. When targeted, inhibition of integrin $\alpha 6$ led to a decrease in self-renewal potential, proliferation, and tumor initiation capacity²⁸. In work by Chintala et al. (1996), it was shown that integrin $\alpha 3\beta 1$ could modify MMP-2 induction and influence tumor cell invasiveness in GBM²⁹.

Bsg-2 is also implicated in the process of angiogenesis, both MMP-dependent and -independent, promoting increased nutrient exposure and utilization by a tumor³⁰. Such an ability would be necessary for metastatic cell survival upon arriving in a new location within the body. This process was evidenced by the abolition of blood vessel formation *in vitro* when Bsg-2 was subjected to RNAi to block its function. This relationship is further investigated in the work by Voigt et al. (2009) where knockdown of Bsg-2 reduced the

expression of vascular endothelial growth factor (VEGF) that promotes the formation of blood vessels that could supply a tumor with the blood flow it requires³¹. The relationship between Bsg-2, MMPs-1, -2, and -9, and angiogenesis was investigated in a melanoma cancer model, where it was noted that MMP-2/9 expression occurs independent of Bsg-2³². However, upon knockdown of Bsg-2, melanoma cells displayed a reduced ability to metastasize to other sites and lost a significant degree of neovascularization. MMPs-2 and -9 are shown to be expressed in human GBM tumors, where they correlate with VEGF and tumor vascularization³². In a human clinical model, GBM tumors taken from patients showed a high degree of correlation between Bsg-2 expression and tumor grade³³. Along with that finding, the expression of Bsg-2 protein was also positively correlated with VEGF and Mevalonate Diphosphate Decarboxylase (MVD), both angiogenic factors. Patients with early stage tumors showed low expression of Bsg and VEGF/MVD, whereas high grade gliomas possessed high levels of all three³³. Work published in 2000 by Sameshima et al. indicated that Bsg-2 could be found in the human brain only in vascular endothelial cells in healthy tissue, but not in actively proliferating vascular tissue in GBMs²⁵. Taken as such, an indirect means for promoting vascularization via MMP induction by Bsg might be implicated in neoplastic GBM tissue.

Increased blood flow derived from the interaction between Bsg, MMPs, and VEGF will allow tumor cell populations to gain better access to energy supplies, namely in the form of glucose molecules to use for ATP synthesis. One trademark of cancer is the process of aerobic glycolysis. The synthesis of ATP energy stores during the process of glycolysis ordinarily results in the production of two pyruvate molecules from a single

glucose molecule. When this process occurs without sufficient oxygen present in cells, such as during strenuous exercise or rapid tumor cell growth, pyruvate is converted to the waste product lactate requiring it to be exported from the cell. In tumor tissue, the cells will only undergo glycolysis, even in the presence of oxygen. This phenomenon is known as the Warburg Effect, after the work performed by Dr. Otto Warburg. With the constitutive aerobic glycolysis, cancerous cells need to uptake glucose at a significantly increased rate compared to normal cells, needing to process a massive amount of the sugar monomers to produce enough ATP to proliferate and spread³⁴. As lactate builds up within the cells, the intracellular space begins to acidify, leading to organelle and cytoskeletal degradation and eventual cell death³⁵. In cancerous tissue, cells will exhibit increased monocarboxylate transporter levels, particularly MCTs 1 and 4, of which Bsg is a chaperone³⁶⁻³⁸. MCTs are large transmembrane proteins with 12 transmembrane domains. In the cell membrane, Bsg will associate with the MCT protein, acting as a “pseudo-subunit”. The association between the two molecules is believed to be the result of charged interactions between amino acids on either protein. Basigin contains a conserved glutamate residue at the 218th amino acid position, where MCT expresses two possible candidates that could facilitate this association³⁷. Within the third transmembrane domain of MCT-1, there are two arginine residues at position 86 and 302 that show the potential to bind to the negatively charged glutamate, but there isn’t enough evidence to declare what amino acids are actually responsible³⁷. Bsg-2 is required to chaperone MCTs bound to lactate molecules to the cell surface from the inside of the cell³⁸. As such, cancerous cells, including GBM, that overexpress Bsg-2 at the cell surface have an increased capacity to remove waste products and protect themselves³⁶⁻⁴⁰.

In Bsg-2-null mice, it was observed that in retinal pigment epithelial cells, MCT-1, -3, and -4 levels were lost without the expression of Bsg-2⁴⁰. The work by Marchiq et al. (2015) outlined the importance of Bsg-2 in stabilizing the function of MCTs-1 and -4 in the role of glycolytic tumor growth and survival³⁹. In later work, it was shown that genetic disruption of Bsg-2 in glycolytic tumor cells was shown to decrease functional levels of the MCTs in the plasma membrane^{39, 40}. Further work using function-blocking antibodies against Bsg in colon cancer and melanoma cells caused necrotic cell death, as opposed to apoptosis due to increased intracellular pH and decreased ATP levels⁴¹. In the same study, normal fibroblast cells weren't subjected to the same cell death, inhibited glycolysis, and obstructed disposal of waste as cancerous cells. This phenomenon is due to the fact that cancerous cells rely on glycolysis to obtain their ATP energy, whereas the normal healthy cells perform oxidative phosphorylation⁴¹.

Basigin-2 is also known to associate with cyclophilins (Cyphs)⁴². These molecules, found both internally and externally, act as receptors for immunosuppressants, modulators of inflammatory responses, and trafficking proteins inside of cells. In certain cancers, CypA, a natural ligand for Bsg, is highly expressed⁴². In the work by Min Li et al., (2006) exogenous CypA was found to stimulate cell proliferation in a pancreatic cancer cell model, mediated by binding to Bsg in a dosage dependent manner, stimulating the ERK1/2 and p38 signaling pathways⁴³. In other work, it was found that binding of Bsg to Apolipoprotein D, a 29kDa secreted chaperone protein, was competitively abrogated by binding of CypA to Bsg⁴⁴. Basigin expression is also known to be affected by Cyp60⁴⁵. Cyp60 binds to Bsg at proline-211 at the transmembrane domain, directly adjacent to the ECD of Bsg. When bound to the Bsg, Cyp60 regulates Bsg expression on

the cell surface, modulating the targeting of the Bsg protein⁴⁵. Despite previous research into the relationship between Cyps and Bsg in cancer, there is little evidence that the two interact within the brain.

In their 2008 publication, Belton et al. synthesized a 24-25kDa recombinant form of human Bsg-2 (rBsg), comprised of the extracellular domain (rBsg-ECD) of the protein attached to a histidine tag¹. The protein was synthesized using a bacterial expression vector that expressed the protein in the periplasmic space between the cell wall and internal cell membrane of the bacteria. In this oxidizing environment, the recombinant protein is able to form stable disulfide bridges due to the non-reducing state of the periplasm, and can be isolated using an osmotic shock lysis method. The rBsg protein mimics the biological activity of the high glycosylated form of natural Bsg-2 so that it cells will recognize the protein as the natural Bsg-2 protein upon binding to the cell surface. This phenomenon is due to the stable tertiary structure of the recombinant protein, illustrating that glycosylation is responsible only in part for the biological activity of Bsg-2. In human uterine endometrial cells, rBsg was shown to induce ERK1/2 phosphorylation through binding to human Bsg-2 at the cell surface¹. When activated via phosphorylation, ERK1/2 phosphorylates transcription factors that cause cell cycle progression and cell survival^{46, 47}. There is also evidence that the MAPK pathway does indeed play a role in tumor survival through oncogenes co-opting ERK1/2 into deregulating Bcl-2 proteins that contribute to cell survival⁴⁸. rBsg was shown to bind to other, unknown receptors besides Bsg-2, illustrating a degree of uncertainty as to what protein rBsg stimulated the cells through¹. Bsg-Bsg binding-mediated ERK1/2 activation, which is normally seen in response to growth factors in a healthy cell

population, is of much significance. It signifies that in a tumor microenvironment, where nutrients are being depleted at a high rate, this signaling pathway can still be activated in tumor cells, which can then push their cell cycles forward and proliferate using the Bsg-mediated ERK1/2 phosphorylation, potentially facilitating some of the previously discussed mechanisms. Since GBM cells express high levels of intramembranous Bsg-2, there is the potential that vesicular shedding of Bsg-2 can induce a pro-survival autocrine/juxtacrine signaling loop within a cancer cell population.

The MAPK signaling pathway is regulated through the EGFR receptor at the surface of cells. In normal cells, after ligand binding, the EGFR protein will activate a signaling cascade, starting with the activation of Ras protein. Once Ras is activated, it phosphorylates the Raf protein, which in turn phosphorylates MEK, a serine/threonine/tyrosine kinase (Fig. 1). Activated MEK in turn will activate ERK1/2 by adding a phosphate group onto the threonine-202/185 and tyrosine-204/187 residues on the ERK1/2 protein⁴⁶. ERK1/2 is composed of two proteins that weigh 44kDa and 42kDa. The protein normally functions as a serine/threonine kinase that adds phosphate groups to transcription factors to activate them and stimulate mRNA and protein production to drive the cell cycle forward and promote nucleic acid synthesis⁴⁷. Normally, ERK1/2 is sequestered in the cytoplasm, preventing its function⁴⁸. Once ERK1/2 is phosphorylated is translocated to the cell nucleus where it phosphorylates numerous transcription factors, including ELK, STAT, c-JUN, and c-FOS. When these factors become active, they promote cell survival and cell cycle progression⁴⁹. In cells where the MAPK pathway has been mutated and is constitutively activated, the cells can grow out of control, promoting the development of cancer⁵⁰. EGFRvIII is a mutated form

of the normal EGFR protein. However, it is missing most of the extracellular domain and is constitutively sending growth signals into the cell, promoting the increased activity of ERK1/2⁶. Degraded ECM proteins produced by Bsg-2 mediated MMP activation can also stimulate EGFR signaling by binding to the cell surface in the tumor microenvironment, potentiating a juxtacrine signaling loop (Fig 2)¹⁵. In the work by Grass et al. (2013), it was shown that Bsg-2 and EGFR are found in close proximity in lipid rafts that interact to drive forward cell invasiveness in a breast cancer cells, establishing a firmer base for investigating the effects of Bsg-2 stimulation of the EGFR-MAPK pathway in GBM cells²¹.

The phytoalexin resveratrol (RSV) is a polyphenol commonly found in grapes, berries, and some species of pine tree. Normally, the molecule is produced in plants in response to stress, where it acts on numerous effectors to decrease stress-induced damage⁵¹. This is believed to occur due to the activation of sirtuins by RSV, which allows for cell growth signals to be transduced, mitigating stress-related damage⁵². RSV has been shown to inhibit the activation of ERK1/2 *in vitro* in mammalian cells, where it also acts as an inhibitor of the downstream effectors of ERK1/2 such as c-JUN, c-FOS, and other transcription factors as well^{53, 54}. However, it was determined that ERK1/2 could be hyperphosphorylated in response to RSV treatment in a chronic myeloid leukemia cell model, indicating a potential variance of effect between tissue types⁵⁵. RSV also has the ability to promote the reversal of TMZ resistance by acting on the NF-κB pathway to reduce the activity of O⁶-methylguanine DNA-methyltransferase (MGMT)⁴. Further, RSV possesses the ability to inhibit or activate cell cycle kinases, and other proteins, such as WAF/p21, to stop cell cycle progression at the G1-phase, force

cancerous cells out of the S-phase, and can reverse hyper-phosphorylation of the Rb tumor suppressor⁵⁶. High concentrations alone were cytotoxic beyond a 60 μ M concentration when given to cells *in vitro*, possibly due to the endocytosis of the RSV, which was determined to cause the activation of multiple signaling pathways culminating in apoptosis in colon cancer and leukemia cells, as well as inhibition of the MAPK pathway^{4, 53, 57}. RSV also has the ability to inhibit MMPs-2/9, VEGF, and EGFR, which, as stated previously, are found in human GBM cells^{51, 54, 58}. RSV can act as an estrogen agonist, as well as an antagonist to the aryl hydrocarbon nuclear receptor, but neither function would be significant enough exert RSV's inhibitory, anti-inflammatory, and pro-tumor suppressor effects⁵⁹. The exact mechanisms for these actions are largely unknown, and there is a lot of evidence pointing in multiple directions. However, in the work by Colin et al. (2011), it was determined that RSV enters cells at lipid rafts in the membrane via clathrin-independent endocytosis, where it was also shown that ERK proteins accumulate after RSV exposure⁵⁷. This could indicate the inhibition of receptors that would otherwise stimulate ERK1/2 phosphorylation. This proposition is supported by the discovery that, when introduced to cells, RSV antagonizes the EGFR-dependent phosphorylation of ERK1/2, which can in turn, downregulate the expression of Bsg-2, and the fact that RSV endocytosis activates pro-apoptotic cell signaling pathway activation^{53, 57, 58}. EGFR, as discussed earlier, is commonly found in lipid rafts. RSV was also found to reduce GBM cell invasiveness, however, not through the EGFR pathway discussed^{60, 61}. While it has been shown that RSV will inhibit ERK1/2 activation in cells treated with PMA, an inducer of ERK1/2 phosphorylation, it hasn't been investigated whether or not RSV will inhibit ERK1/2 activation in GBM cells that are treated with

rBsg or even fetal bovine serum (FBS), which has been shown to activate the protein kinases^{1,53}. This project sought to establish the relationship between rBsg treatment of human GBM cells, MAPK pathway activation, and ERK1/2 inhibition via resveratrol.

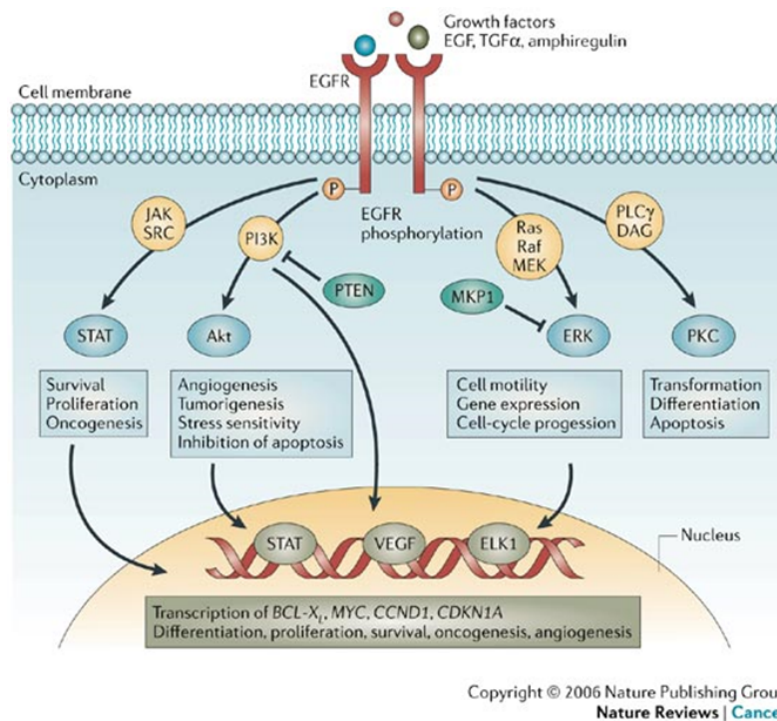


Figure 1: The EGFR receptor transduces signals along multiple signaling pathways. Once activated, EGFR proteins become phosphorylated and activate the EGFR/Ras/ERK1/2 signaling pathway, along with others, that drives gene expression, cell motility, and cell-cycle progression. Activation of ERK1/2 causes phosphorylation of ELK1, which in turn transcribes genes responsible for proliferation and cell survival. Taken from “Integration of EGFR inhibitors with radiochemotherapy” by Nyati et al., 2006, *Nature Reviews Cancer*, Vol. 6, pg. 876-885. Copyright 2006 by Nature Publishing Group. Used with permission.

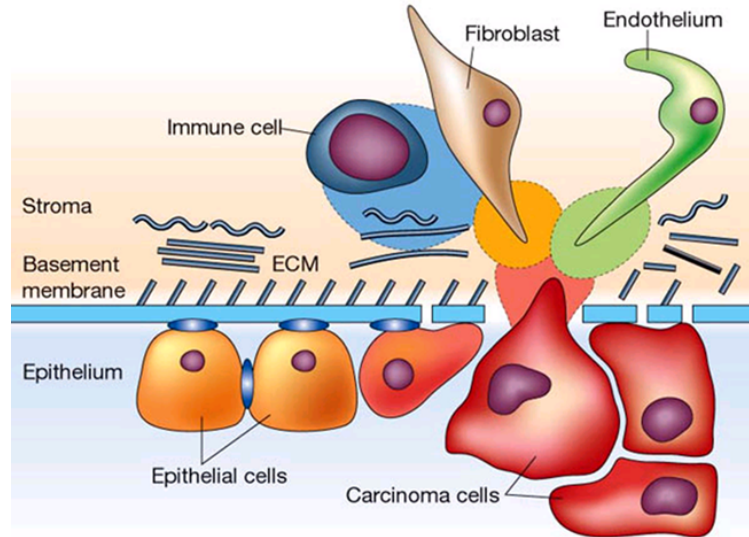


Figure 2: Mechanism for tumor cell invasion. The basement membrane produced by normal stromal and endothelial cells serves as a physical barrier to the metastasis of cancer cells within the body. Extracellular matrix proteins found in the basement membrane and the ECM are broken down by enzymes called matrix metalloproteinases. This enzymatic action causes a break in the basement membrane, allowing cancerous cells to spread. Taken from “The microenvironment of the tumor-host interface” by L.A. Liotta and E.C.Kohn, 2001, *Nature*, Vol 411, pg. 375-379. Copyright 2001 by Nature Publishing Group. Used with permission.

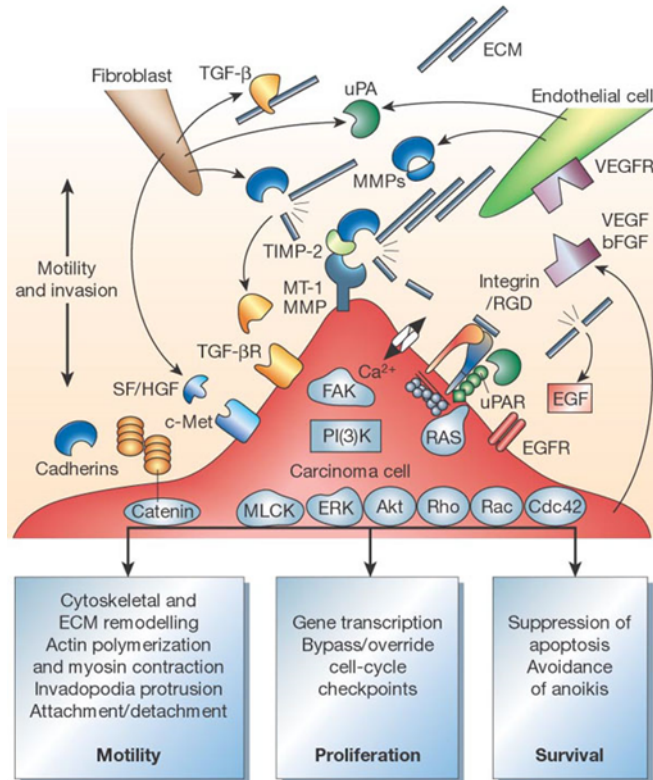


Figure 3: Molecular communication at the tumor invasion front. MMPs released from both normal endothelial and fibroblast cells can be stimulated by the release of signaling molecules from cancerous cells such as VEGF, bFGF, and Bsg-2 (not pictured). MMP mediated degradation of ECM proteins causes activation of the EGFR signaling pathway in the cancerous cells, signaling the cells to begin dividing. Taken from “The microenvironment of the tumor-host interface” by L.A. Liotta and E.C. Kohn, 2001, *Nature*, Vol 411, pg. 375-379. Copyright 2001 by Nature Publishing Group. Used with permission.

AIMS AND GOALS

Glioblastoma multiforme is the most common malignant form of human brain cancer, characterized by an aggressive nature and poor prognosis. GBM, unlike normal brain tissue, expresses high levels of the protein Basigin-2 (Bsg-2), an Ig-like transmembrane protein with numerous pro-cancer cell signaling properties. It was previously described by Belton et al. (2008) that a recombinant form of human Bsg-2 (rBsg), containing the extracellular domain of the protein, could bind to normal Bsg-2 at the surface of human endometrial stromal cells, stimulating MMP production and activating the EGFR-Ras-ERK1/2 signaling pathway. This pathway, when activated, allows for the transcription of proteins that drive the cell cycle forward and promote cell survival. When the pathway is constitutively activated as is often the case in cancers, uncontrolled cellular growth and proliferation can occur, leading to tumor growth.

I hypothesized that treating human GBM cells with rBsg would cause activation of ERK1/2 by binding to Bsg-2 at the cell surface, illuminating an autocrine/juxtacrine signaling loop used by GBM tumor cells. To accomplish this, rBsg would be produced via a bacterial expression vector containing the sequence for rBsg that the protein could be isolated and purified from. Once sufficient purified protein was isolated, GBM cells would be treated with the rBsg protein, lysed, and analyzed for changes in ERK1/2 phosphorylation. Recombinant Basigin-2 would then be conjugated to a Ultraviolet (UV)

light-activated hetero-trifunctional cross linker that, when exposed to UV light, would transfer a biotin tag from the rBsg “bait protein” to any transmembrane protein that the rBsg had bound to at the cell surface. This would then allow for the isolation of the putative receptors, with Bsg-2 being at the top of the list of those suspected to bind rBsg based off of previous findings. The activation of ERK1/2 by rBsg would then be blocked by the antioxidant phytoalexin Resveratrol (RSV) that has been shown to disrupt ERK1/2 signaling in hopes of establishing a link between RSV and Bsg-2 mediated ERK1/2 signal activation.

METHODS AND MATERIALS

Cell Culture

U87-MG human glioblastoma multiforme cells (ATCC) were obtained from cryostorage from the UMBTC. For propagation, cells were grown in Eagle's Modified Essential Medium (EMEM) (Lonza) + 10% Fetal Bovine Serum (FBS) (Lonza) in 75cm² cell culture flasks. For treatment assays, cells were plated on 35mm, tissue-treated cell culture dishes to allow for ease of access and a uniform cell number when grown to confluency.

Control and Experimental Protein Lysate Collection

All control and treatment cells were grown to confluency in 35mm dishes, achieving a cell count of roughly 1.0×10^6 cells per dish. Prior to any control or experimental treatment, cells were serum starved using serum-free EMEM for 18-24hrs to synchronize their cell cycles and prevent further growth. A time course assay was created to be able to observe a stepwise increase in ERK1/2 activation in the U87 cells, consisting of six treatment periods at room temperature (0sec, 30sec, 1min, 2min, 5min, and 10min) comparing ERK1/2 phosphorylation between unstimulated cells and cells stimulated with FBS or rBsg. The time course was eventually changed to 0min, 5min, 10min, 15min, 20min, and 30min incubation times at 37°C to properly induce the cells.

Control cells were plated, grown to confluency, and serum starved for 18-24hrs prior to treatment. Unstimulated control cells were treated for the allotted time periods with serum-free EMEM at 37°C. Stimulated cells were treated with EMEM+10% FBS for the allotted time period at 37°C. Once each treatment was completed, cells were lysed with 0.5mL ice-cold 1% NP-40 lysis buffer and placed on ice for five minutes. A cell scraper was used to collect all cell material and debris to one edge of the 35mm dish. The mixture of lysis buffer and cellular material was transferred to a labeled 1.5mL centrifuge tube and vortexed vigorously to ensure complete lysis. All centrifuge tubes containing cell lysates were centrifuged at 21000x the force of gravity (g) for 10min at 4°C. The supernatants were removed and transferred to separate, clean 1.5mL centrifuge tubes and placed on ice. Lysates were immediately subjected to a BCA (ThermoFisher) assay to determine protein concentration according to the manufacturer's protocol. All lysate samples were stored at -20°C. A separate set of control cells were subjected to resveratrol (RSV) (TCI America) treatment to inhibit ERK1/2 phosphorylation. It was determined through Western Blot analysis that cells would be given a 2hr pre-treatment of 30µM RSV and a co-treatment of 30µM in the appropriate treatment media. Control cells to be treated with RSV were serum starved for 18-24hrs prior to the addition of RSV. Each dish of cells was given serum-free EMEM+30µM RSV for 2hrs and incubated at 37°C. Cells were then given either serum-free EMEM+30µM RSV (Unstimulated cells) or EMEM+10% FBS+30µM (stimulated) for the allotted time period. The treated cells were then washed and lysed under the same conditions as non-RSV-treated control cells and subsequently subjected to a BCA assay. These lysates were stored at -20°C.

Bacterial Cell Culture

The expression vector BL-21RP *E. coli* bacteria were the gift of Dr. Belton for use in the isolation of recombinant human basigin-2 (rBsg) from a glycerol stock, stored at -80°C. These cells contained the pASK-IBA44 plasmid containing the sequence for rBsg with a polyhistidine tag, and ampicillin (Amp) and chloramphenicol (Chl) resistance genes. Bacteria were streaked directly onto an LB agar plate containing 100µg/mL ampicillin and 34µg/mL chloramphenicol and grown overnight at 37°C in the dark.

rBsg Isolation

A single colony of BL-21RP cells containing the rBsg plasmid was picked and used to inoculate 5mL of LB broth+Amp+Chl. The inoculated LB broth was grown overnight at 37°C in the dark at 200rpm on a shaker. The overnight culture was streaked onto two LB+Amp+Chl agar plates. These plates were grown overnight at 37°C in the dark. Exposure to light does not affect protein expression. A single colony from the overnight cultures was used to inoculate 5mL of SOC media (2% w/v tryptone, 0.5% w/v yeast extract, 8.56mM NaCl, 2.5mM KCl, d_4H_2O to 1000mL, 10mM MgCl₂, 10mM MgSO₄, 20mM glucose) containing 100ug/mL Amp and 34µg/mL Chl, which was allowed to culture for 5hrs at 37°C in the dark. Four milliliters of the pre-culture were added to 200mL SOC media containing 100µg/mL Amp and 34µg/mL Chl in a 1L Erlenmeyer. The newly inoculated 200mL of SOC was allowed to culture for 12hr at 200rpm at 37°C in the dark. Four 1L Erlenmeyer flasks were filled with 200mL of SOC containing 100ug/mL Amp. Fifty milliliters of the overnight SOC culture were added to each of the four 1L Erlenmeyer flasks containing SOC+Amp. These were allowed to culture for 1hr at room temperature at 200rpm. After 1hr, 25µL of 2mg/mL

anhydrotetracycline (ACROS) in dimethylformamide were added to each of the cultures to induce rBsg protein expression. The induced cultures were allowed to continue culturing for 4hrs at room temperature at 200rpm. The entire culture volume was transferred, on ice, to 50mL conical tubes (twenty tubes in total) and centrifuged at 3220xg for 10mins at 4°C in an Eppendorf 5810 centrifuge with a swinging bucket rotor. The supernatant was decanted off and the wet weight of the bacterial cell pellet was measured. Twenty five milliliters of Sucrose buffer (30mM Tris-Cl pH 8.0, 20% w/v sucrose) was added to each pellet and each pellet was thoroughly resuspended. Fifty microliters of 0.5M EDTA (pH 8.0) were added to each tube and mixed. The bacterial suspensions were allowed to incubate on ice for 10mins. The tubes were centrifuged at 3220xg for 20mins at 4°C. The supernatant was decanted off and 25mL of MgSO₄ buffer (5mM MgSO₄) were added to each pellet and each pellet was resuspended. The bacterial suspensions were allowed to incubate on ice for 10mins before being centrifuged at 3220xg for 20mins at 4°C. The supernatants of each osmotic shock lysate (OSL) tube, which contained rBsg protein, were consolidated into a single 500mL bottle and stored at 4°C and on ice until it was ready to be concentrated. Four Millipore 10K centrifugal filters (Sigma-Aldrich) were obtained and chilled on ice. Fifteen milliliters of OSL were added to each filter tube. The filter tubes were then centrifuged at 3220xg at 4°C and a starting time of 20mins, which gradually increased as more protein was collected. This was repeated until the entire 500mL OSL sample was concentrated to roughly 4mL. The OSL in each centrifugal filter was then washed with 15mL 1X Wash Buffer (300mM NaCl, 50mM NaH₂PO₄ pH 8.0) three times until the concentration of MgSO₄ was <0.0015mM. A 50µL sample of OSL was saved for BCA and SDS-PAGE analysis. The

final OSL concentrate was collected using a 20-200 μ L Eppendorf Research Plus micropipettor and stored at -20°C. To purify the rBsg sample, two milliliters of cobalt Talon Affinity Beads (G-Biosciences) in 50% ethanol suspension were aliquoted into a 15mL conical tube and centrifuged at 1000xg for 2mins at 4°C. The beads were washed 3 times with 15mL 1X Wash Buffer (used earlier), centrifuged at 1000xg for 2mins at 4°C, and the supernatant was discarded between each wash. After the final wash, the OSL sample was added to the beads and placed in a rotator at 4°C for 2hr. The beads were centrifuged at 1000xg for 2mins at 4°C. The supernatant was removed and stored at -20°C in a 15mL conical labeled “Unbound rBsg Purification Fraction” for BCA and SDS-PAGE analysis. The beads were washed with 10mL Ni-NTA Buffer (1X Wash Buffer, 5mM Imidazole, 0.5mM PMSF) and centrifuged at 1000xg for 2mins at 4°C. The supernatant was removed and stored at -20°C in a 15mL conical labeled “rBsg Purification Wash #1” for BCA and SDS-PAGE analysis. The beads were washed two more times with 10mL Ni-NTA Buffer. The beads were suspended in a final 10mL Ni-NTA buffer and were added to a 15mL column. The beads were allowed to settle and the Ni-NTA buffer was allowed to move through the matrix until the meniscus reached the top of the beads. Five more milliliters of Ni-NTA buffer were added and allowed to run through the column to wash the beads. Ten milliliters of Elution Buffer (1X Wash Buffer, 200mM Imidazole, 0.5mM PMSF) was added to the column and allowed to move through the matrix. The eluent was collected in a single 15mL conical. The purified rBsg sample was concentrated using two more Millipore 10K centrifugal filters. The final concentrated, purified rBsg was stored indefinitely -20°C.

rBsg Treatment of U87-MG Cells and Protein Lysate Collection

U87-MG cells were plated in 12, 35mm culture plates and allowed to grow to confluency. rBsg generated during my purifications would be used for the following experiments. The cells were serum-starved for 18-24hrs prior to treatment. Six plates would be used for rBsg monotreatment and the other six would be given a combination treatment of rBsg and RSV. Cells that were to be given RSV treatment were incubated with 30 μ M RSV in serum-free EMEM for 2hr at 37°C prior to time course treatments. Conditioned media was warmed in a 37°C water bath prior to the assay. Working with one set of experimental plates at a time, the media was aspirated off of the cells and 1mL serum-free EMEM containing 10 μ g/mL rBsg or 10 μ g/mL rBsg+30uM RSV was added to each plate and one of each was allowed to incubate for 5min, 10min, 15min, 20min, 30min, or 60min, one plate from each treatment condition for each time period. At the conclusion of the given time period, the conditioned media was aspirated off and 0.5mL ice-cold 1% NP-40 lysis buffer (20 mM HEPES buffer [pH 7.0-7.4] 1% NP-40, 0.5% Sodium Deoxycholate, 150 mM NaCl, 2 mM EDTA pH 8, 2.5 mM Sodium Pyrophosphate) was added to the cells. The plates were rocked to spread the detergent and were placed on ice for at least 5mins. A cell scraper was used to collect all cell material and buffer to one edge of the plate. All material inside the plate was transferred to a clean, chilled, and labeled 1.5mL centrifuge tube using a micropipettor and vortexed vigorously to ensure complete lysis. Lysates were placed on ice until all plates for a given had been processed. All lysates were centrifuged at 21000xg at 4°C for 10mins. The supernatant from each tube was transferred to a correspondingly labeled, chilled 1.5mL centrifuge tube and stored at -20°C. Lysates were subjected to BCA analysis according to

the manufacturer's specification to determine protein concentration for use in SDS-PAGE and Western Blot analysis.

Sulfo-SBED rBsg Binding Assay

An aliquot of rBsg protein was obtained from Dr. Belton for this assay due to time constraints, at a concentration of 1.7mg/mL in 0.5mL in a 1.5mL microcentrifuge tube and stored at 4°C until ready to use in the label transfer assay. Sulfo-SBED biotin label transfer reagent (ThermoScientific) was obtained and one "No-Weigh" microtubule of reagent was opened, in the dark, and mixed with 22uL of DMSO until dissolved. In the dark, 11µL of dissolved Sulfo-SBED reagent was added to the 0.5mL of rBsg protein and incubated at room temperature for 30mins. Five Slide-A-Lyzer dialysis units (ThermoScientific) were allowed to soak in ice-cold dH₂O for 15mins before usage. A beaker was filled with ice-cold PBS and a magnetic stir bar and was placed inside a cooler filled with ice. The dialysis units were filled with 100uL of labeled protein and placed into a float which was then placed into the ice-cold PBS and allowed to dialyze for 2hrs in the dark. Once the dialysis was complete, the purified rBsg-SBED samples were transferred to individual 1.5mL centrifuge tubes, containing roughly 170µg of protein in each and were stored at -80°C.

U87-MG cells were grown in six 35mm plates until confluent. The old media was removed and the cells were washed with PBS (Lonza). The PBS was removed and the cells were given 3mL of pre-warmed serum-free EMEM and were incubated overnight at 37°C. Three treatment groups were used for the label transfer assay: untreated cells exposed to UV light in a UV Stratalinker (Stratagene) for 5mins at a 5cm distance at max power, 5min treatment with rBsg-SBED in serum-free EMEM at 37°C prior to exposure

to the UV light, and a 10min treatment with rBsg-SBED at 37°C before treatment with UV light. In a dark cell culture hood, the serum-free media was aspirated, and the cells were washed with PBS. After aspirating the PBS, pre-warmed serum-free EMEM containing 30µg/mL of rBsg-SBED was added and the cells were allowed to incubate. Once the incubation was complete, the cells were immediately transferred to the UV Stratalinker, with the lids off, and exposed to UV light for 5mins at a distance of 5cm at maximum power. The cells were removed from the Stratalinker and placed in the cell culture hood. The media was aspirated and saved and the cells were washed with PBS thoroughly. The cells were given 0.5mL of ice-cold 1% NP-40 lysis buffer (20 mM HEPES buffer [pH 7.0-7.4] 1% NP-40, 0.5% Sodium Deoxycholate, 150 mM NaCl, 2 mM EDTA pH 8, 2.5 mM Sodium Pyrophosphate), which was rocked to spread it evenly across the cells, and transferred to ice for 5mins. The lysates were collected using a cell scraper to scrape all cellular material to one edge of the 35mm plate, where they were collected using a micropipettor to a pre-chilled and labeled 1.5mL microcentrifuge tube, which was stored on ice until all lysates were prepared. Untreated cells were given only serum-free EMEM prior to UV light exposure. All lysates were vortexed vigorously and then centrifuged for 10mins at 4°C at 21000xg in an Eppendorf 5810R tabletop centrifuge. The supernatant of each lysate was transferred to a new, pre-chilled and appropriately labeled 1.5mL centrifuge tube and stored at -20°C until ready to use. The label transfer assay was performed once more, using the same methods, with treatment media containing 120µg/mL rBsg-SBED. All lysates were subjected to SDS-PAGE and Western Blot analysis. The second set of lysates, exposed to 120µg/mL of rBsg-SBED, was run in duplicate gels along with serial dilutions of pure rBsg-SBED alone at 1/10,

1/100, and 1/1000 concentrations of the stock rBsg-SBED. One gel was exposed to reducing conditions, while the other one was non-reduced.

Western Blot Analysis

Treated U87-MG lysates were subjected to SDS-PAGE with 10ug of protein per well in BioRad Mini-PROTEAN TGX 4-15% gels with 50uL wells and were allowed to run at 150V until the dye front began to move off of the gels. Proteins were transferred (Transfer buffer composition: 25mM Tris-Cl, 192mM glycine, pH 8.3, 20% methanol, 0.1% w/v SDS) at a constant 0.10A for 10hrs at RT onto PVDF membranes. All blots were blocked with 20mL of 5% Non-fat Dry Milk (NFDM) in Tris-Buffered Saline + 0.1% Tween-20 (TBST) (50mM Tris, 150mM NaCl, 0.1% w/v Tween-20 [ThermoFisher]) for 1.5hrs at room temperature with gentle rocking. Primary antibodies were diluted in TBST to the appropriate concentration in 20mL for each membrane and incubated on the membranes for 1.5hrs at room temperature with gentle rocking. Primary Ab solution was decanted off of the membranes and 20mL of TBST was added to wash the blots three times for 10mins each. Secondary antibodies were diluted in TBST to the appropriate concentration in 20mL for each membrane and incubated on the membranes for 1.5hrs with gentle rocking. The secondary Ab solution was decanted off and 20mL of TBST was added to wash the blots three times for 10mins each. West Pico ECL reagent (ThermoFisher) was prepared during the final wash. Four milliliters of ECL reagent was added to each blot and allowed to incubate at room temperature for 5mins. The membranes were sealed in saran wrap and secured in an imaging cassette. The membranes were exposed to film for 2sec, 10sec, 30sec, 5min, and overnight. Exposed film was processed by a Kodak X-Omat Film Processor in the UMBTC Dark Room.

ERK1/2 antibodies were purchased from Cell Signaling Technologies. Basigin-Extracellular Domain (ECD) antibodies were synthesized and obtained from stocks prepared by Dr. Belton. Antibodies used: RAH anti-pERK1/2 (1:2000) (Cell Signaling), RAH anti-ERK1/2 (1:1000) (Cell Signaling), MAH anti-EMMPRIN-ECD (1:1000), MAH anti-Hsp90 (1:1000), GAR-HRP secondary Ab (1:25000), GAM-HRP secondary Ab (1:20000) (ThermoFisher). NeutrAvidin-HRP (ThermoScientific) was used for imaging lysates from the Sulfo-SBED label transfer assay at two dilutions based off of the supplier's recommendations (1:20000, 1:4000).

RESULTS

Recombinant Basigin Isolation, Purification, and Analysis

It was hypothesized that rBsg protein, described in Belton et al. (2008), could stimulate the ERK1/2 signaling pathway in U87-MG human GBM cells. In order to obtain rBsg, it had to be produced in a bacterial expression vector that would allow for quick production of large amounts of the protein. The rBsg, in order to maintain its demonstrated biological activity, needed to be expressed in the periplasmic space of the BL21 *E. coli* bacteria. The periplasm of the bacteria has an oxidizing environment, causing the disulfide bridges between the Bsg-ECD cysteine residues to form. BL21 *E. coli* transformed with the pASK-IBA44 plasmid containing the sequence for rBsg were grown in culture overnight in a warm room. The following day, bacterial rBsg protein expression was induced with 2mg/mL anhydrotetracycline for 4hrs at room temperature. Osmotic shock lysates containing the recombinant protein were obtained and concentrated to purify the rBsg, which were incubated with cobalt beads to bind the histidine tag on the rBsg for affinity chromatography. The cobalt beads have an affinity for histidine residues, in this case, at the C-terminal end of the recombinant protein. When the rBsg was incubated with the beads, the poly-histidine tags bound to the cobalt beads, pulling the protein out of the Ni-NTA buffer solution. During the chromatography,

any unbound material can be washed off before adding the elution buffer, allowing for the isolation of pure protein off of the beads. Once the rBsg was purified, it was able to be analyzed for its purity by SDS-PAGE and Western blotting.

The initial preparation of the rBsg protein revealed that most of the recombinant protein was eluted in the first four 1mL fractions, with the largest amount coming out after the second 1mL of eluent (Fig. 4A lane 4). As the elution fractions were collected, less and less protein was observed in the SDS-PAGE gels (Fig. 4A lanes 5-8, Fig. 1B lanes 2-6). In lane 7 of Fig. 4B, the unbound fraction collected after the cobalt bead incubation contained a large amount of rBsg not bound to beads, indicating an issue with the rBsg-to-bead binding.

The first two rBsg isolation preparations and purifications revealed issues with the purification protocol that led to incomplete purification of the concentrated osmotic shock lysate (Fig. 1-2). The estimated size of the rBsg protein is 24.0kDa. Prominent bands in the “unbound” fractions in lanes 3 and 5 at the same weight as the purified rBsg indicate that not all of the rBsg was bound to the cobalt beads. To remedy the immediate problem, the unbound fractions were incubated with more cobalt beads and subjected to affinity chromatography, isolating more, but not all of the rBsg. The third preparation differed from the others in that during the cobalt bead incubation, the beads/sample were placed in a rotator in a 4°C cold room. It was believed that incubating the recombinant protein with the cobalt beads for a longer time and a colder temperature would promote higher yields. SDS-PAGE analysis revealed a much greater purification of the protein than seen before (Fig. 6).

The first two preps were combined to make a sample with a protein concentration of 810ng/ μ L and a final volume of 650 μ L. Serial dilutions were made of the combined first two preparations of rBsg protein, ranging from 810ng/ μ L down to 0.081ng/ μ L, diluting by ten-fold at each dilution step for the purpose of testing the sensitivity of Coomassie staining and the West Pico Enhanced Chemoluminescence (ECL) imaging system (ThermoFisher), as well as for the presence of purified rBsg protein. The ECL reagent contains a chemical known as luminol, which, upon reaction with an oxidating agent such as HRP, will produce blue light. When imaging film is exposed to the light and subsequently developed and fixed, a black mark will appear on the film, indicating the presence a protein targeted by the Western blot. Coomassie staining will detect proteins as long as a given protein's concentration is above 100ng/ μ L. This leads us to expect a lack of bands for all samples below that 100ng/ μ L concentration. One microliter of each dilution was run out onto each of two SDS-PAGE gels. One gel was stained with Coomassie brilliant blue (Fig. 7), revealing only a single band in the 810ng well. The other was subjected to Western blot analysis and probed for the presence of the rBsg protein (Fig. 8 rBsg). The results of this test would indicate that the bands seen in Coomassie stained gels are indeed rBsg, further proving that purified recombinant protein was isolated. Visible bands were observed in the 810ng, 81ng, and 8.1ng wells, with the intensity of the bands decreasing as the amount of protein decreased. The lack of bands in the 0.81ng and 0.081ng wells indicates that the chemiluminescent substrate isn't able to detect concentrations that low. The larger molecular weight band in the 810ng lane indicates the presence of dimers between rBsg molecules, an expected result given the natural ability of normal Bsg-2 to form homodimers^{1,9,10,14}. After the completion of the

rBsg analysis, all three preparations were combined into a single sample and were concentrated down to a final volume of 1.5mL with a concentration of 458.2µg/mL, or roughly 0.6873mg of purified rBsg.

Early Control Cell Lysate Collection Attempts

In later experiments, rBsg protein would be given to U87 cells in an attempt to stimulate ERK1/2 phosphorylation. In order to be able to draw any conclusion from the results of said experiments, there would need to be a control to compare the results to. Normally, cells are exposed to numerous growth factors and nutrients, both *in vivo* and *in vitro*, which cause the stimulation of the ERK1/2 pathway because it is employed by both healthy and cancerous cells. In cell culture practices, fetal bovine serum (FBS) and other nutrient sources are used to allow cells to grow and divide, partly by stimulation of the ERK1/2 pathway. This trait was used to compare the effects of rBsg protein to FBS to observe if the recombinant protein could mimic the ERK1/2-stimulatory effects.

Prior to the establishment of a control cell lysate collection and analysis protocol, numerous western blots were performed in an attempt to establish pERK1/2 levels in serum stimulated U87-MG cells. All lysate collections were performed after a time course of treatment with EMEM+10%FBS where cells were exposed to FBS for 0sec, 30sec, 1min, 2min, 5min, and 10min prior to lysis. SDS-PAGE and Western blot analysis were performed on the lysates, however, very little usable data come out of all of the different attempts (Early serum treated U87 lysates, Fig 9-12). Most blots performed had incomplete transfers, resulting in the absence of a molecular weight standard protein ladder to use in sample identification (Fig 9-11). Some blots showed nonspecific binding of the secondary antibody to the molecular weight standards, causing the presence of

large smears on the ladder (Fig. 12-13). Most blots showed large smearing of sample bands. Jurkat cells obtained from Cell Signaling Technologies were run out on an SDS-PAGE gel and subjected to Western blot analysis (Fig. 13). These cells were used in an attempt to diagnose if the problems with imaging stemmed partly from the U87-MG lysates that I had prepared. The two vials of Jurkat T-cell lysates, obtained from Cell Signaling Technologies, expressed either pERK1/2 levels or no ERK1/2 phosphorylation, acting as positive and negative controls respectively. The blot itself was somewhat interpretable, leading to the observation that negative control Jurkat cells in lane 2, cells that contained no ERK1/2 phosphorylation, showed no banding at the estimated molecular weight of the ERK1/2 protein, while the positive control Jurkat cells did show pERK levels in lane 3 (Fig. 13). These cells were not used for any other experiments after the issues with the Western blotting protocol used were fixed. It was later determined that the failure of the preliminary blots were, in part, due to the use of improper antibody dilution buffers that inhibited proper protein labeling.

Antibody Nonspecific Binding Test Assay

After the issues with the Western blot protocol were fixed by obtaining the correct dilution buffers and minor technique changes, all of the antibodies to be used needed to be tested for nonspecific binding under this new protocol. In some cases, some antibodies will show some specificity to proteins with similar amino acid compositions, causing an antibody designed to detect one target protein to bind to an off-target protein, skewing the results and showing signal where there should not be any. This can occur with both primary and secondary antibodies. Primary antibodies should only bind to the protein that they were raised up against. Secondary antibodies should only bind to any antibodies

produced in the host that they are targeted against. To accomplish this, SDS-PAGE was performed on U87-MG cell lysates that were either unstimulated or stimulated with 10% FBS in EMEM for 5mins, having been given only serum-free EMEM. These lysates were then subjected to all of the antibodies that would be used during the course of the experiment (Fig. 14). The purpose of this experiment was to test to make sure that our primary antibodies worked (Fig. 14A) and that there was no nonspecific binding of our secondary antibodies to anything on the PVDF membranes (Fig. 14B). All of the primary antibodies worked, and neither of the secondary antibodies exhibited nonspecific binding.

Resveratrol Treatment Assay

The antioxidant phytoalexin resveratrol was selected as an inhibitor of ERK1/2 phosphorylation based on previous works⁵¹⁻⁵⁹. RSV is also shown to act through the ERK1/2 signaling pathway to inhibit Bsg-2 expression, making the molecule an even more interesting player in terms of experimenting with the relationship between ERK1/2 signaling and Bsg-2⁵³. Prior to establishing control cell lysates, the appropriate method of RSV treatment needed to be determined. A 200mM stock solution of RSV in 100% ethanol was prepared for use in treating U87-MG cells. In prior work performed by Huang et al. (2008), cells incubated with RSV 2hrs prior to treatment and lysis showed ERK1/2 phosphorylation inhibition⁵³. Other works used direct treatments in conjunction with other substances⁵⁶. To address this variance in RSV treatment, U87-MG cells were grown in culture and treated with different conditions of 30 μ M RSV to determine the most effective method of inhibiting ERK1/2 phosphorylation (Fig 15). Performing this test would allow for the first observation of how RSV acts upon ERK1/2 phosphorylation in response to stimulation with naturally occurring growth factors, mimicking a body's

natural environment.. Unstimulated cells given only serum-free EMEM showed no decrease in the levels of phosphorylated ERK1/2, as did unstimulated cells incubated for 2hrs with 30 μ M RSV in serum-free EMEM prior to being given only serum-free EMEM (Fig. 15, Lanes 1 and 2). Unstimulated cells were used to test to see if RSV had any effect on total ERK1/2 levels. Given the nature of cancer cells, some ERK1/2 phosphorylation was expected to be seen, especially if the cells expressed the EGFRvIII protein, which, as described earlier, constitutively produces signals down its effector pathways. Control cells stimulated for 5mins with 10% FBS, only, in EMEM showed the highest levels of ERK1/2 phosphorylation (Fig 15. Lane 5). Cells stimulated with 10% FBS in EMEM in the presence of 30 μ M RSV after a 2hr pre-treatment with RSV in serum-free EMEM showed the greatest amount of ERK1/2 inhibition when compared with control cells stimulated in the absence of RSV (Fig 15. Lane 7). After analysis of the blot using the NIH ImageJ software, it was found that ERK1/2 phosphorylation in cells pre- and co-treated with RSV was 8.2% that of cells given only FBS (Fig. 16). Due to this finding, it was decided that for all RSV treatments, cells would be given a 2hr pre-treatment with 30 μ M RSV in serum-free EMEM and a 30 μ M RSV co-treatment at the time of experimental condition treatment.

Unstimulated Baseline ERK1/2 Phosphorylation in U87-MG Cells

U87-MG cells were given serum-free EMEM treatment to establish baseline levels of ERK1/2 phosphorylation if there was any during the time course (Fig. 17). The western blot revealed that the levels of ERK1/2 phosphorylation are consistent when given only serum-free media. However, these cells were incubated at room temperature

during the initial time course that was developed with time points of 0sec, 30sec, 1min, 2min, 5min, and 10min.

Serum-Stimulated ERK1/2 Phosphorylation in U87-MG Cells

As previously stated, it was hypothesized that rBsg, when given to human GBM cells, could stimulate the ERK1/2 signaling pathway. Once activated, ERK1/2 phosphorylates numerous transcription factors that promote cell survival and cell cycle progression in not only healthy cells, but in tumor cells as well, usually to a much higher degree. In order to establish a positive control for rBsg treatment, U87-MG cells were treated with 10% FBS in EMEM to stimulate ERK1/2 phosphorylation in what are normal, *in vitro* culture conditions which would then be compared to the level of phosphorylation seen in cells treated with only rBsg. Cells were treated with the serum containing media during two different time courses and incubation temperatures. The first consisted of time periods of 0sec, 30sec, 1min, 2min, 5min, and 10min at room temperatures (Fig. 18). The second time course consisted of longer periods of 0min, 5min, 10min, 15min, 20min, and 30min at 37°C (Fig. 19). The initial experiment was considered inaccurate due to the fact that it was performed at room temperature. In order for the results of the experiment to be considered accurate, it was decided that the conditions needed to mimic the body's internal conditions, thus the switch to 37°C. The first time course experiment showed a time-dependent increase in ERK1/2 phosphorylation in responses to the serum treatment. When performed in the presence of RSV, there is a substantial reduction of ERK1/2 activation. The exposures to film shown in Fig. 18 are of different exposure length due to overexposure of the film to the blots of RSV-free treatment conditions at the same exposure time as the treatments containing

RSV, as indicated. The second time course revealed similar results. However, rather than a continual increase in ERK1/2 phosphorylation as seen in Fig. 18., a peak in pERK1/2 levels is seen between 10min and 15min after the addition of the treatment media, followed by a steady plateau in later time periods. This signifies that the cells have reached peak ERK1/2 phosphorylation where the maximum amount of signal is being produced. The effects of the RSV are also similar to those seen in the first time course. The RSV treatment mitigated the peak phosphorylation event at the 10min period to 50.2% of the non-inhibited cells, an event not observed during the first time course (Fig. 19, Fig. 20). The RSV was also shown to lose its effect at longer exposure times, indicated by the increasing intensity of the pERK1/2 bands seen on the blot. This could be due to the uptake of RSV into the cells. As more of the RSV is pulled out of solution and is processed by the cells, the less of an effect it can produce, however, this is just speculation. The images seen in Fig. 19 were obtained at the same exposure length, illustrating a better comparison between the two experimental groups.

rBsg Treatment of U87 Cells

Now that control levels of ERK1/2 phosphorylation in response to serum-treatment had been established, U87-MG cells were grown in culture and prepared for treatment with rBsg protein grown during the purification attempts performed for this work. In this experiment, purified protein was dissolved into serum-free EMEM media and given to cells in the same manner as the serum-containing media in an attempt to observe if the hypothesized interaction would occur. Giving cells only rBsg in serum-free EMEM is necessary because any observed phosphorylation of ERK1/2 would mean that the rBsg alone was responsible for the signal activation. Similar to the control cells, two

differing time courses were used, one with shorter incubation times at room temperature, and the other with longer incubation times at 37°C. The initial set of lysates was deemed inaccurate, leading to the formation of the second time course (Figure 21). This inaccuracy was due to incubating cells at room temperature rather than 37°C. For Bsg-2 to begin stimulating cells, it must be endocytosed by cells at lipid rafts. In order for that interaction to happen, the conditions need to be correct. Since no observed phosphorylation occurred, it was hypothesized that room temperature, roughly 20°C, was far too low for the endocytosis of the rBsg to occur. For both time courses, the U87 cells were treated with either 10µg/mL rBsg in serum-free EMEM or 10µg/mL rBsg+30µM RSV after a 2hr pre-treatment with 30µM RSV. After completion of the first time course assay, there was no increase in ERK1/2 phosphorylation observed (Fig. 21). Similarly, no real changes or trends could be observed in the blot containing lysates from cells treated with rBsg and RSV, providing little insight into the relationship between the two (Fig. 21). During the second time course, the cells were exposed to their treatment for longer periods of time at 37°C rather than 20°C. These changes illustrated a better relationship between rBsg and ERK1/2 phosphorylation. The lysates obtained from this time course showed an increase in ERK1/2 phosphorylation with a strong peak between 10min and 15min, similar to the serum-stimulated U87 lysates, although, rather than a plateau in signaling, there is a sharp drop off in signaling, mostly likely due to the loss of rBsg available to cause stimulation of the ERK1/2 proteins (Fig. 22), however, this is speculation. In the cells treated with rBsg and RSV, there is a 23.7% decrease of rBsg-mediated ERK1/2 phosphorylation at the peak phosphorylating event at 10mins (Fig. 23). Unstimulated cells showed no pERK1/2 when exposed to rBsg in any of the samples.

Different from the serum-stimulated cells, there is no increase in ERK1/2 activation in the later time periods.

Sulfo-SBED Label Transfer Assay

After observing that rBsg does indeed cause ERK1/2 stimulation, it was hypothesized that the rBsg was binding to normal human Bsg-2 at the surface of the cancer cells, along with others potentially. In order to test this, a way of identifying the putative receptors for the rBsg was needed. Purified rBsg protein was incubated with a molecule known as Sulfo-SBED (ThermoFisher) that would bind to rBsg via an NHS ester. The molecule consists of the amine reactive NHS ester, a UV light-activated aryl azide group, a cleavable disulfide spacer arm, and a transferable biotin tag. The molecule works by being conjugated to a “bait protein”, using its NHS ester group, by incubating the bait protein with the Sulfo-SBED. This conjugation does not affect the bait protein’s binding capabilities. When labeled bait protein is put into solution and given to cells, the protein can bind to receptors at the surface of the cells. Then, the cells are exposed to UV light, which causes the aryl azide to transfer the biotin tag to the receptor protein. This will only occur when a bait protein is bound to its receptor, not while floating free. After exposure to denaturing agents such as SDS, DTT, and heat, the disulfide spacer arm will be cleaved, leaving the biotin tag to be completely transferred to the receptor. Once the biotin tag is fully transferred to the receptor, it can be identified by using a NeutrAvidin-HRP (ThermoFisher) detection protein and ECL reagent during Western blot analysis of treated cell lysates. U87-MG cells were treated with rBsg attached to the Sulfo-SBED. Cells were exposed to the labeled protein for two different time periods, similar to the simple rBsg treatments described earlier, but after the incubation was completed, the cells

were exposed to UV light for 5mins at a 5cm distance and at the maximum power of the Stratalinker 1800 instrument in order to activate the crosslinker and transfer the biotin tag to anything that was bound to the rBsg-SBED. Lysates treated with 30 μ g/mL rBsg-SBED were tested for the presence of the biotin tag using NeutrAvidin-HRP protein (ThermoScientific), the Bsg-2 extracellular domain using an antibody raised up against rBsg, and phosphorylated ERK1/2. Western blot analysis revealed only single bands in the 5min and 10min exposures at roughly 26kDa in NeutrAvidin-HRP blots at the 1:4000 dilution of the protein (Fig. 21). This indicates that only rBsg was biotinylated, signifying an issue with either label transfer or self-dimerization of the rBsg, which has been known to happen¹. The lysates showed activation of ERK1/2 in all treatment groups, indicating a stimulus caused by the rBsg-SBED (Fig. 22). The Bsg-2 extracellular domain was also identified with bands at roughly 26kDa and 50kDa, the latter of which only being visible after a 5min film exposure prior to film processing (Fig. 22). The other set of lysates, exposed to 120 μ g/mL rBsg-SBED, were run out on SDS-PAGE gels as either denatured or non-denatured samples, alongside three serial dilutions of the stock of rBsg-SBED protein at dilutions of 1/10, 1/100, and 1/1000 (Fig. 23). The purpose of the denatured vs. nondenatured samples was to see if cleavage of the disulfide spacer arm was actually occurring. These gels were only probed with NeutrAvidin-HRP. Nonreduced samples should have had intact biotin tags, whereas reduced rBsg-SBED should have had no biotinylation when probed with NeutrAvidin-HRP. In the denatured gel, all lysate samples only showed the presence of biotinylated rBsg (Fig. 23). This observation signifies that there is still an issue with the bait protein, most likely self-dimerization. The serial dilutions only showed a doublet band at in the 1/10 dilution of the stock rBsg-

SBED protein, indicating that there is still rBsg protein with the biotin tag. The denaturation should have caused the dissociation of the rBsg with the SBED molecule. In the non-denatured gel, the rBsg-SBED is detected in all lysate samples used, indicating no label transfer to any molecule other than the rBsg. The serial dilutions have visible bands in the 1/10 and 1/100 dilutions while the 1/1000 lane shows nothing (Fig. 23). All bands in the non-denatured gels moved farther down the gel due to not being fully denatured.

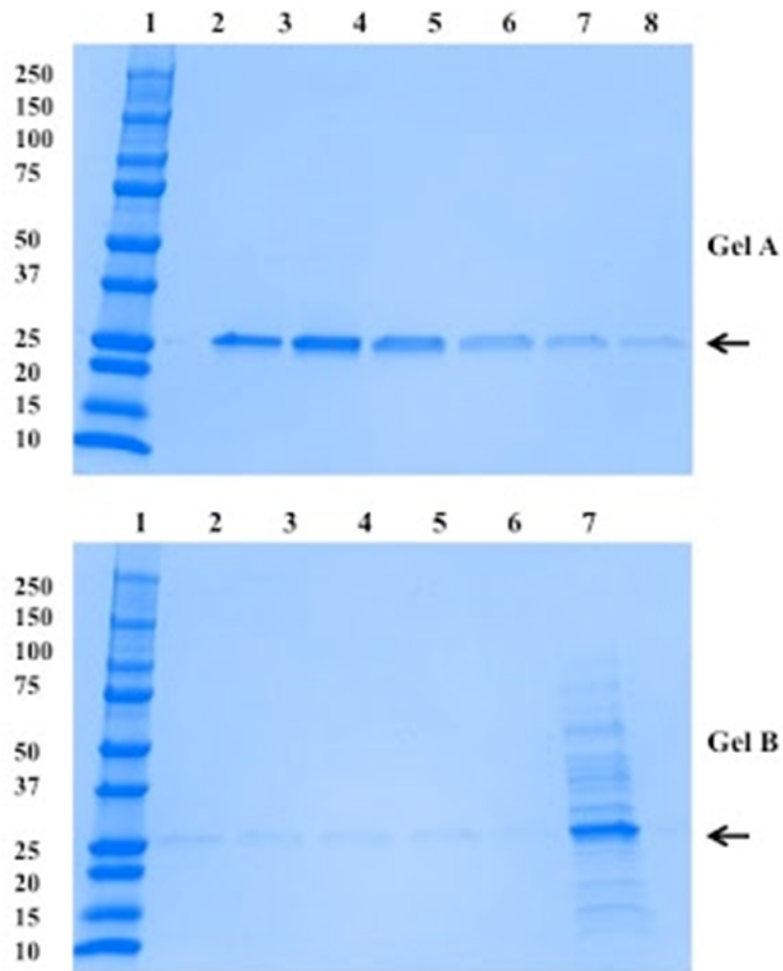


Figure 4. SDS-PAGE analysis of rBsg-ECD elution fractions. The rBsg-ECD protein was purified using cobalt agarose affinity chromatography beads and analyzed by coomassie staining of SDS-PAGE gels. Protein fractions were eluted from a column using 200mM imidazole in phosphate buffer and collected as 1mL samples. 10 μ L samples of each fraction were resolved through 4-15% TGX SDS-PAGE gels, and the gels were stained with coomassie brilliant blue. Eluted fractions are shown in lanes 2-8 in gel A and lanes 2-6 in gel B. The purified rBsg-ECD protein is visible at ~26kDa (arrow). Lane 7 in gel B represents the “unbound” material following affinity purification, indicating that some rBsg-ECD remained in this fraction following purification. The molecular weight standards are shown in lane 1 in each gel and the values shown on the left represent their molecular mass in kilodaltons (kDa).

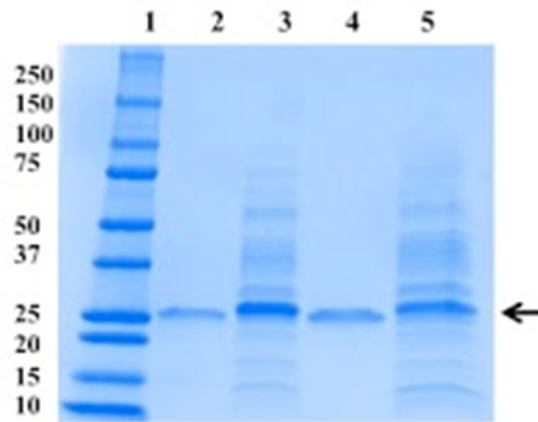


Figure 5. SDS-PAGE of concentrated rBsg-ECD and unbound protein fractions. The purified protein produced from the first two attempts at affinity purification were concentrated and desalted using 10K MWCO centrifugal filters (Millipore). Lanes 2 and 3 show the purified and concentrated rBsg-ECD protein and the unbound fraction from the first prep; Lanes 4 and 5 show the purified and concentrated rBsg-ECD protein and the unbound fraction from the second prep. The prominent bands in lanes 3 and 5 (arrow) indicate that a significant amount of the rBsg-ECD was not recovered during purification. The molecular mass of the protein standards shown in lane 1 are listed on the left in kilodaltons (kDa).

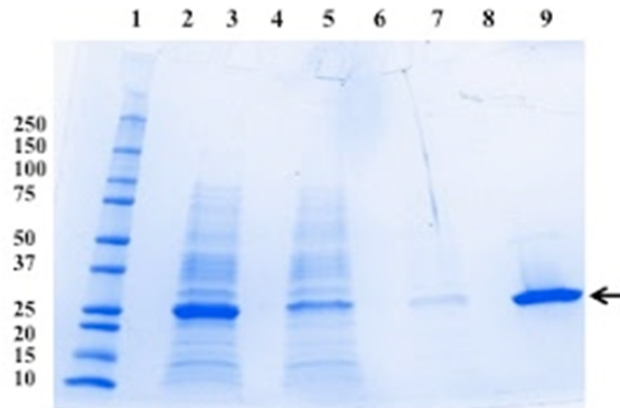


Figure 6. SDS-PAGE of final rBsg-ECD purification. The rBsg-ECD protein purification procedure was modified in order to improve recovery of the recombinant protein, This included using a longer incubation of the osmotic shock lysate with cobalt beads at 4°C on a rotator mixer. Compared to the previous purification attempts shown in figures 1 and 2, there appears to be a reduced amount of rBsg-ECD in the unbound fraction (lane 5), and a greater amount of purified protein collected (lane 9) than there was in the previous attempts. Lane assignments: Lane 3 = osmotic shock lysate, Lane 5 = unbound fraction, lane 7 = first wash fraction of column, Lane 9 = Purified rBsg-ECD. The molecular mass of the protein standards shown in lane 1 are listed on the left in kilodaltons (kDa).

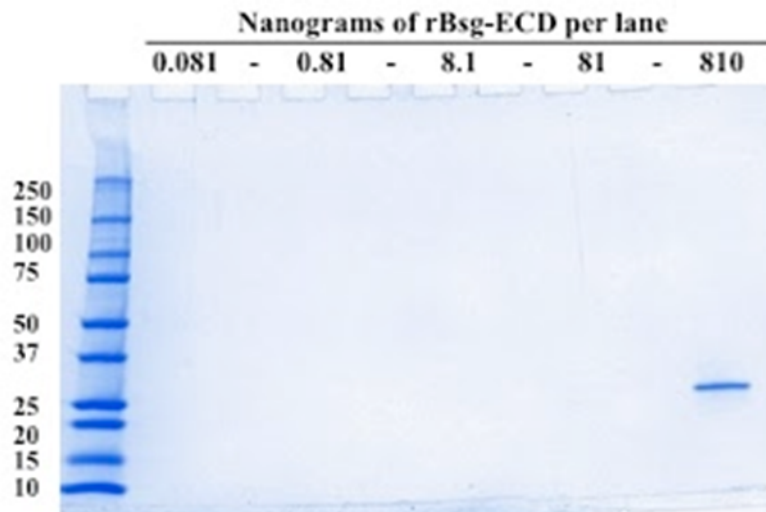


Figure 7. Coomassie blue stained SDS-PAGE of serial diluted rBSG-ECD. Ten-fold dilutions of concentrated rBsg-ECD were prepared and the indicated amounts of rBsg-ECD in nanograms were resolved by 4-15% SDS-PAGE. The top of the figure indicates the mass of protein present in each lane. Note that there are blank lanes containing no protein in the alternating lanes (-). The recombinant protein is visible only in the lane containing 810ng of protein because of the limit of detection for the dye. The molecular mass of the protein standards shown in lane 1 are listed on the left in kilodaltons (kDa). Please see figure 5 for the immunoblot analysis of duplicate gels.

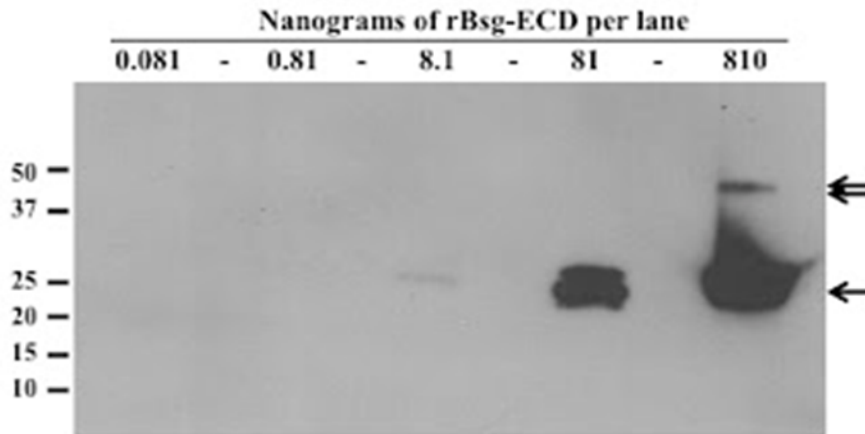


Figure 8. Basigin immunoblot analysis of rBsg-ECD dilution series. Ten-fold dilutions of concentrated rBsg-ECD used in Figure 4 were resolved by 4-15% SDS-PAGE. The top of the figure indicates the mass of protein present in each lane. Note that there are blank lanes containing no protein in the alternating lanes (-). Following transfer of the proteins to PVDF membrane, the blot was probed with a 1:1000 dilution of the P2C2-1-D11 monoclonal antibody (Belton 2008). A commercial goat anti-mouse HRP-conjugated secondary antibody (Thermo Scientific) was used at a 1:20,000 dilution to detect the primary antibody, and blot treated with the Pierce Pico Chemiluminescence Reagent to detect the labeled proteins (Thermo Scientific). Film was exposed to the membrane for 3 seconds and then processed using a Kodak X-Omat film processor. The immunoblot blot analysis revealed the presence of an rBsg-ECD monomer (single arrow) and an rBsg-ECD dimer (double arrow) in the lane containing 810ng of protein. It should be noted that the immunoblot could detect as little as 8ng of the protein.

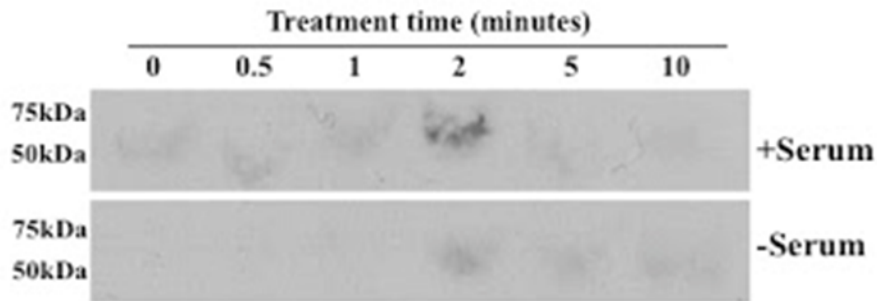


Figure 9. Analysis of ERK1/2 expression in U87MG cells. U87MG cells were treated with either serum-free culture media (bottom) or culture media containing 10% fetal bovine serum (top) for the time periods shown. Cell lysates were resolved by SDS-PAGE and processed for immunoblotting to detect the extracellular regulated kinases 1 and 2 (ERK1/2) with a rabbit anti-ERK1/2 monoclonal antibody diluted 1:1000, and an anti-rabbit IgG HRP-conjugate diluted 1:1000 (Cell Signaling Technologies). Images were obtained using the Pico Chemiluminescent Substrate (Thermo Scientific) and a Kodak X-Omat film processor. While some signal is apparent, the results failed to detect the expected proteins at 42 and 44kDa.

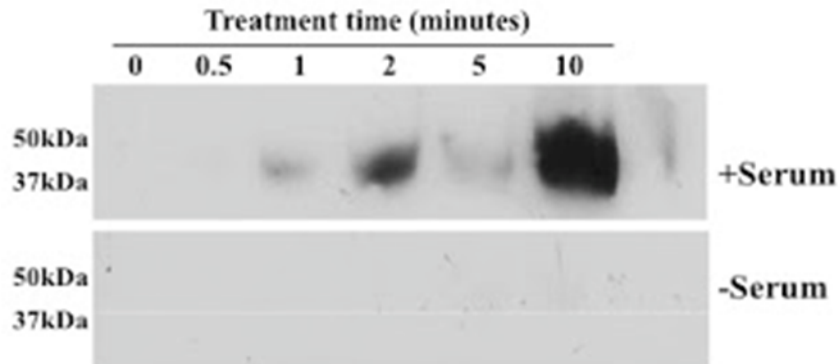


Figure 10. Analysis of ERK1/2 activation in U87MG cells treated with FBS. U87MG cells were treated with either serum-free culture media (bottom) or culture media containing 10% fetal bovine serum (top) for the time periods shown. Cell lysates were resolved by SDS-PAGE and processed for immunoblotting to detect the activation of extracellular regulated kinases 1 and 2 (ERK1/2) with the anti-phosphoERK1/2 monoclonal antibody diluted 1:2000, and the anti-rabbit IgG HRP-conjugate diluted 1:1000 (Cell Signaling Technologies). Images were obtained using the Pico Chemiluminescent Substrate (Thermo Scientific) and a Kodak X-Omat film processor. While there appears to be an increasing amount of signal in response to serum treatment, the results failed to detect the expected individual proteins at 42 and 44kDa.

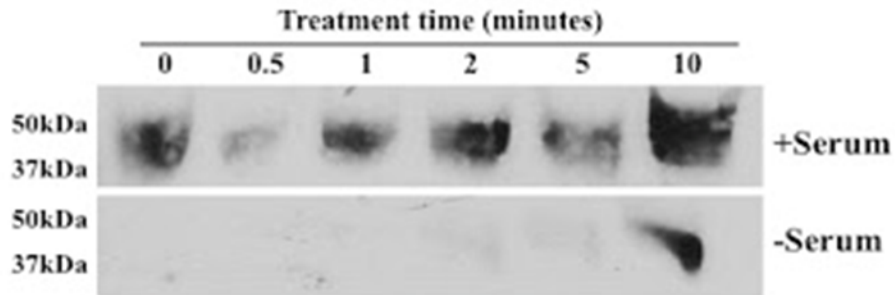


Figure 11. Repeat analysis of ERK1/2 activation in U87MG cells treated with FBS. In an attempt to improve upon the results shown in figure 7, the experiment was repeated. U87MG cells were treated with either serum-free culture media (bottom) or culture media containing 10% fetal bovine serum (top) for the time periods shown. Cell lysates were resolved by SDS-PAGE and processed for immunoblotting to detect the activation of extracellular regulated kinases 1 and 2 (ERK1/2) with the anti-phosphoERK1/2 monoclonal antibody diluted 1:2000, and the anti-rabbit IgG HRP-conjugate diluted 1:1000 (Cell Signaling Technologies). Images were obtained using the Pico Chemiluminescent Substrate (Thermo Scientific) and a Kodak X-Omat film processor. While there appears to be an increasing amount of signal in response to serum treatment, once again the results failed to detect the expected individual proteins at 42 and 44kDa.

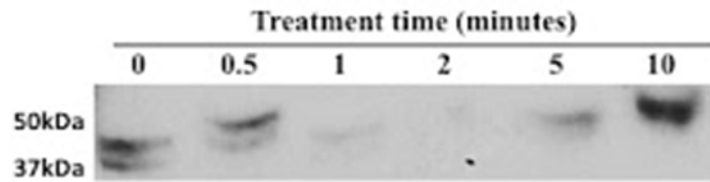


Figure 12. Repeat analysis of ERK1/2 expression in U87MG cells treated with serum-free media. This is a repeat of the experiment shown in the bottom panel of figure 6. U87MG cells were treated with serum-free culture media for the time periods shown. Cell lysates were resolved by SDS-PAGE and processed for immunoblotting to detect the extracellular regulated kinases 1 and 2 (ERK1/2) with a rabbit anti-ERK1/2 monoclonal antibody diluted 1:1000, and an anti-rabbit IgG HRP-conjugate diluted 1:1000 (Cell Signaling Technologies). Images were obtained using the Pico Chemiluminescent Substrate (Thermo Scientific) and a Kodak X-Omat film processor. While the blot shows the expected presence of individual bands, their relative migrations and intensities were not .

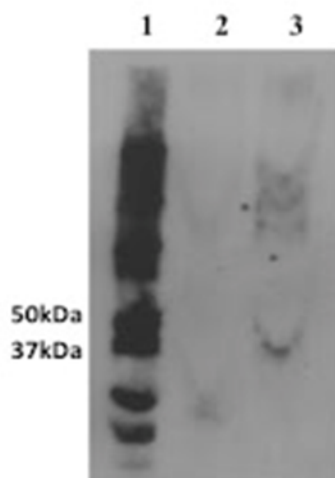


Figure 13. Jurkat T-cell lysate immunoblots for phosphorylated ERK1/2. In an attempt to trouble shoot the lack of results from previous experiments using the anti-phosphoERK1/2 antibody, Jurkat T-cell lysates purchased from Cell Signaling Technologies were resolved by SDS-PAGE and immunoblotted using the anti-phosphoERK1/2 (1:2000). Lane 1 contained the protein molecular weight standard, lane 2 contained the unstimulated Jurkat T-cell lysate, and Lane 3 contained the stimulated Jurkat T-cell lysate. As before, the blots were treated with the Pico Chemiluminescent Substrate (ThermoFisher) and exposed to film for 24 hours. The blot revealed non-specific labeling of the protein ladder in lane 1 and a lack of specific banding in the stimulated Jurkat T-cell lysate (lane 3). The absence of a signal in this positive control lysate indicated that the methods used for immunoblotting were not working.

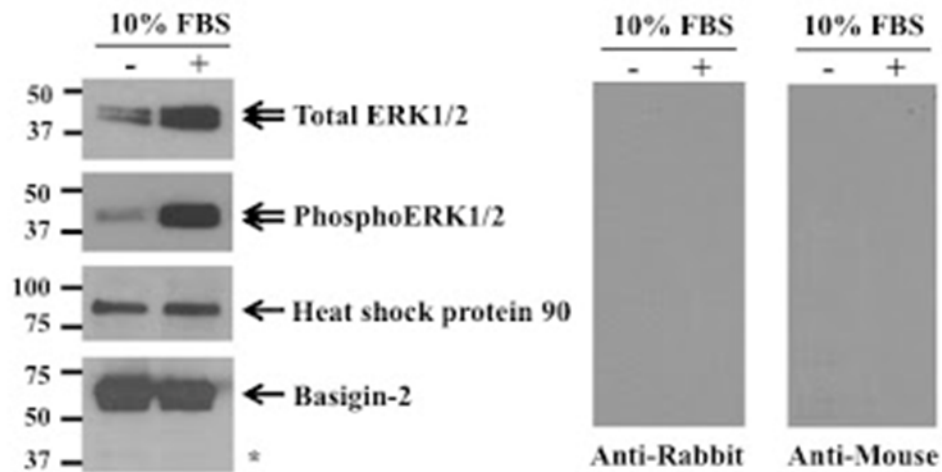


Figure 14. Primary and secondary antibody control immunoblot analysis. Detergent-soluble cell lysates were collected from U87MG cells treated for 5 minutes with cell culture media containing 10% FBS (+), or media lacking FBS (-). Equal amounts of protein were loaded in each lane (20ug) and resolved by SDS-PAGE. Immunoblot analysis was performed according to Belton et al. (2008) using the following four primary antibodies: rabbit anti-human total ERK1/2 (Cell Signaling Technologies; diluted 1:1,000), rabbit anti-human phosphoERK1/2 (Cell Signaling Technologies; diluted 1:2,000), mouse anti-human Hsp90 (Origene; diluted 1:1,000), and mouse anti-human EMMPRIN-ECD (1:1,000). The horseradish peroxidase (HRP) conjugated secondary antibodies used were both from Thermo Scientific: goat anti-rabbit HRP-conjugate (diluted 1:20,000) and goat anti-mouse HRP-conjugate (diluted 1:20,000). The images on the left demonstrate specific labeling of the proteins at the correct molecular weights. The images on the right represent duplicate immunoblots lacking the primary antibodies demonstrating that the signals produced on the left were not a result on non-specific secondary antibody binding. The faint band in the EMMPRIN-ECD blot (labeled with an asterisk *) is the low glycosylated form of human Basigin-2.

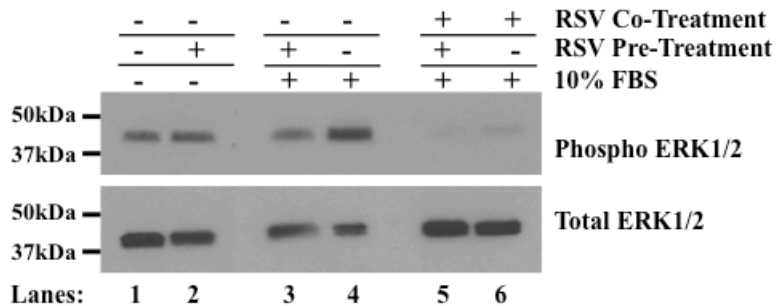


Figure 15. Characterization of the effects of Resveratrol on ERK1/2 activation in U87MG cells treated with FBS. The indicated U87MG cultures (lanes 2, 3, and 5) were pre-treated with 30 μ M RSV in serum-free media for 2 hours prior to treatment with 10% FBS. Lanes 5 and 6 also contained RSV in the treatment media (co-treatment). Following a 5 minute stimulation with 10% FBS (lanes 2-6), the cells were lysed and the lysates subjected to immunoblot analysis using the anti-phosphoERK1/2 primary antibody (1:2000) anti-totalERK1/2 primary antibody (1:1000). Lane Assignments: 1) Unstimulated 2) Unstimulated+RSV pre-treatment 3) Serum-stimulated+RSV pre-treatment 4) Serum-stimulated 5) Serum-stimulated+RSV pre-treatment+RSV co-treatment 6)Serum-stimulated+RSV co-treatment.

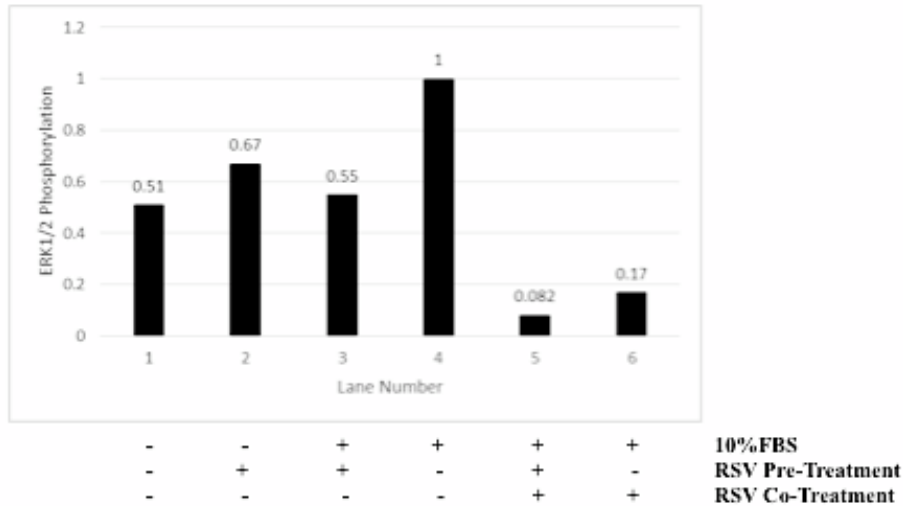


Figure 16. Pre-treatment and Co-treatment of cells with 30 μ M RSV produces the greatest amount of inhibition of FBS-stimulated ERK1/2 activation in U87MG cells. The indicated U87MG cells (Lanes 2, 3, and 5) were pre-treated with 30 μ M RSV in serum-free media for 2hrs prior to lysis (Lane 2) or treatment with 10% FBS (Lanes 3 and 5). Lanes 5 and 6 also contained 30 μ M RSV in the treatment media. Following a 5min stimulation with 10% FBS (Lanes 3-6), the cells were lysed and probed for ERK1/2 phosphorylation levels. The immunoblots were subjected to analysis using NIH ImageJ software. Lane 4 represented the maximum amount of ERK1/2 activation and all values were normalized to that value. The level of ERK1/2 phosphorylation seen represent percent values of the maximum amount of ERK1/2 phosphorylation seen in Lane 4. Cells pre-treated and co-treated with 30 μ M RSV showed the largest degree of ERK1/2 inhibition, showing only 8.2% of the maximum amount of ERK1/2 activation. This method of RSV treatment was selected.

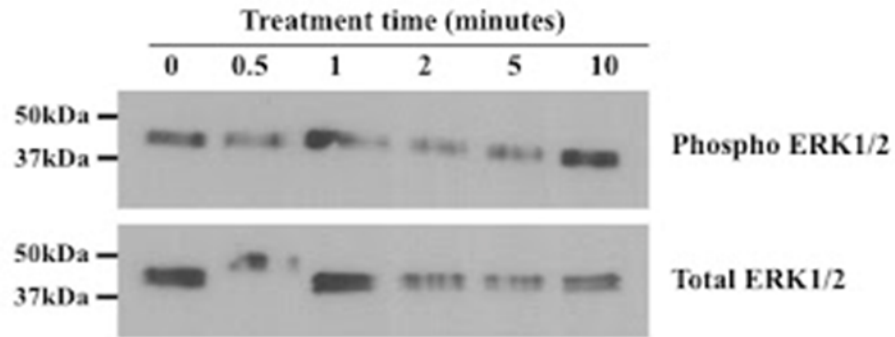


Figure 17. RSV treatment of U87MG cells to determine baseline ERK1/2 expression and phosphorylation levels. U87-MG cells were treated with serum-free culture media containing 30 μ M RSV for the stated time periods in an attempt to detect changes in the level of ERK1/2 phosphorylation and total ERK1/2 protein levels. Following treatment, the cells were washed with cold PBS, lysed and immunoblotted with the anti-phosphoERK1/2 primary antibody (1:2000) or the anti-totalERK1/2 primary antibody (1:1000). The blots were imaged using the Pico Chemiluminescent Substrate (ThermoFisher) and a Kodak X-Omat film processor. These images were obtained from a 10sec exposure to film.

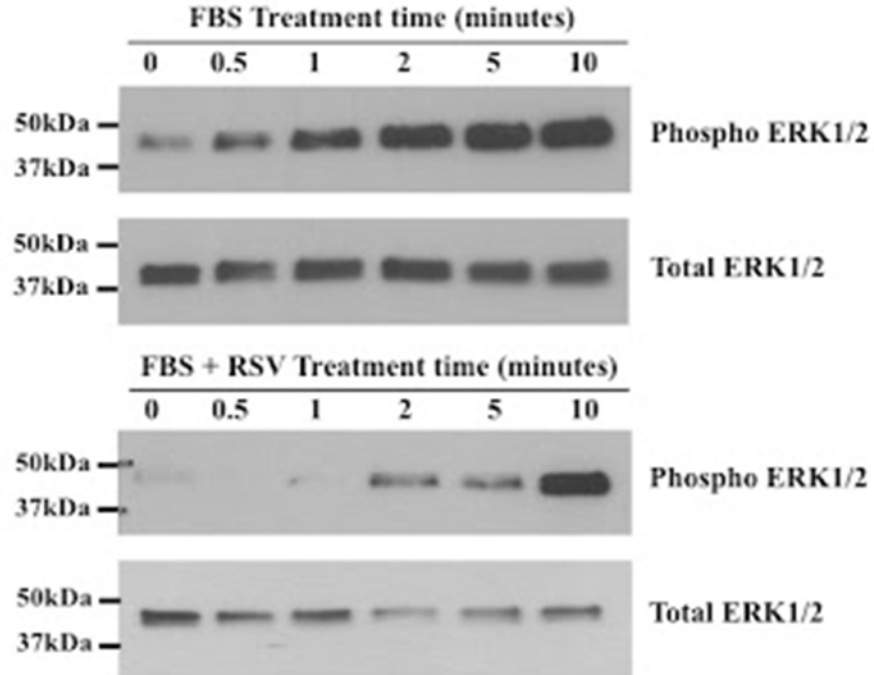


Figure 18. Resveratrol treatment of U87MG cells reduces FBS-induced ERK1/2 phosphorylation at room temperature (21°C). U87-MG cells were treated with cell culture media containing 10% FBS or culture media containing 10% FBS and 30 μ M RSV at room temperature. Following treatment, the cells were washed with cold PBS, lysed and immunoblotted with the anti-phosphoERK1/2 primary antibody (1:2000) or the anti-totalERK1/2 primary antibody (1:1000). The blots were imaged using the Pico Chemiluminescent Substrate (ThermoFisher) and a Kodak X-Omat film processor.

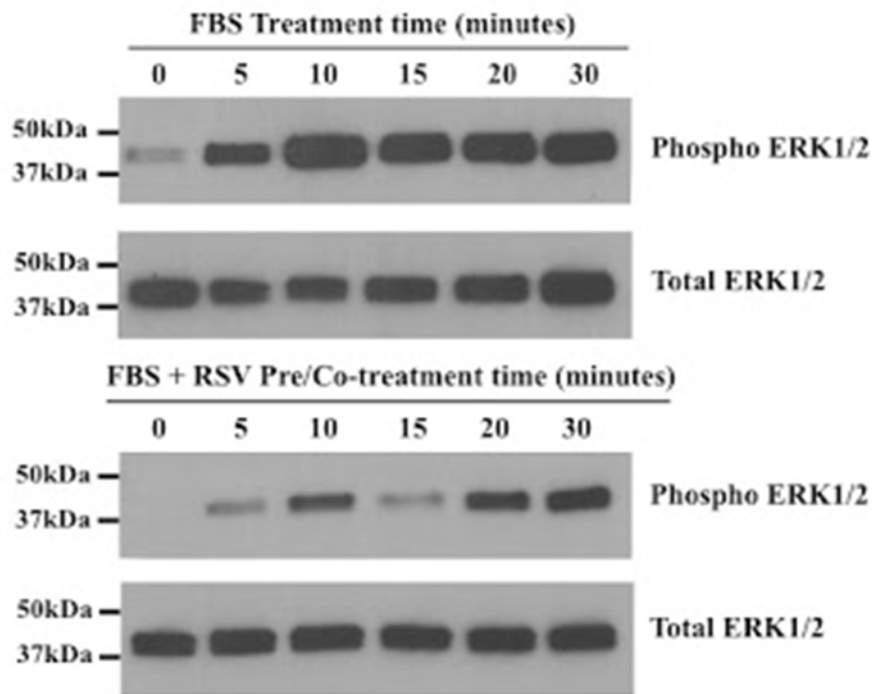


Figure 19. Resveratrol treatment of U87MG cells reduces FBS-induced ERK1/2 phosphorylation at body temperature (37°C). U87-MG cells were treated with cell culture media containing 10% FBS (top) or pre-treated with 30uM RSV for 2 hours and then and treated with culture media containing 10% FBS and 30µM RSV (bottom) at 37°C. Following treatment, the cells were lysed and immunoblotted with the anti-phosphoERK1/2 primary antibody (1:2000) or the anti-ERK1/2 primary antibody (1:1000). The blots were imaged using the Pico Chemiluminescent Substrate (ThermoFisher) and a Kodak X-Omat film processor. These blots revealed a peak phosphorylation event of ERK1/2 occurring at the 10min time interval. The resveratrol treatment reduces serum-stimulated ERK1/2 phosphorylation.

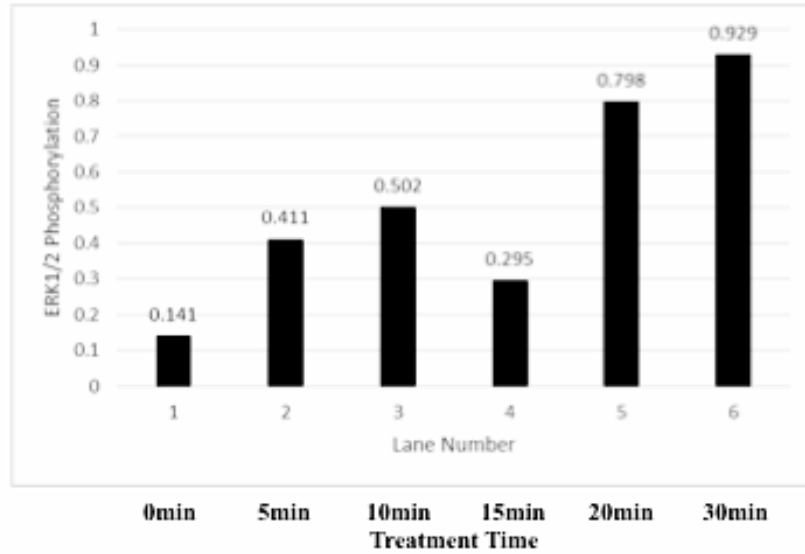


Figure 20. Resveratrol treatment of U87MG cells reduces peak FBS-induced ERK1/2 phosphorylation at body temperature (37°C). U87MG cells were treated with either media containing 10% FBS alone or 10% FBS+30 μ M RSV for the listed time periods prior to lysis. Lysates were probed for ERK1/2 activation to determine the degree of inhibition by RSV. The values listed represent the amount of ERK1/2 phosphorylation seen in cells treated with RSV compared to cells given only FBS at the same time period. The peak phosphorylation event seen in FBS-only treated cells at 10mins is reduced by 49.8%. After the 15min time point, the degree of RSV-mediated ERK1/2 inhibition decreases and ERK1/2 phosphorylation levels begin to closely resemble the FBS-only treated cells at the same time points

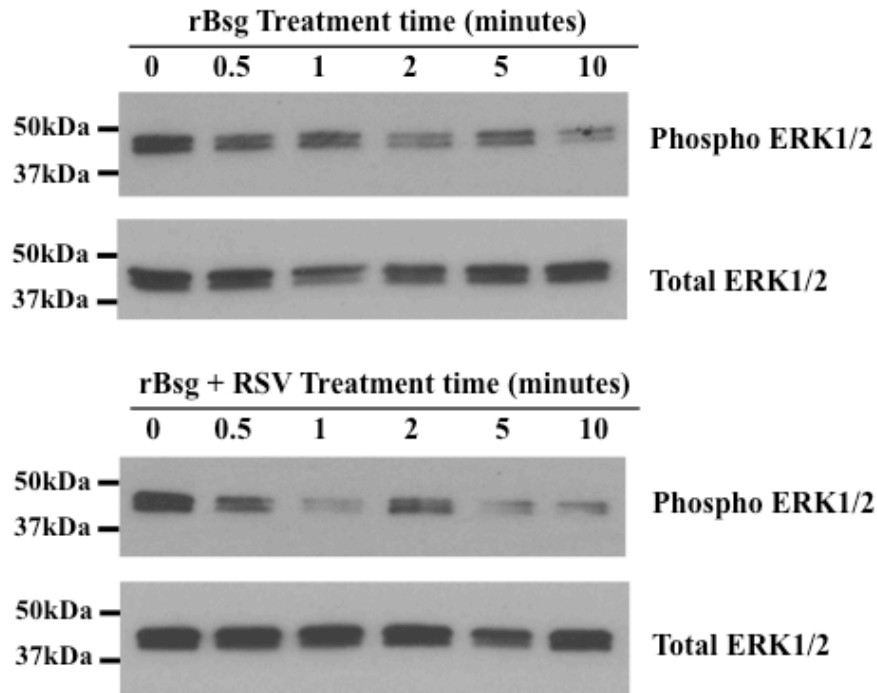


Figure 21. Initial immunoblot analysis of U87MG cells treated with rBsg or rBsg+30 μ M RSV. U87MG cells were treated with either rBsg protein only or rBsg+30 μ M RSV in serum-free EMEM media for the indicated time period at 37°C. Cells were then lysed and the protein fraction was collected and subjected to Western blot analysis. Immunoblotting was performed using the anti-phosphoERK1/2 primary antibody (1:2000) and the anti-ERK1/2 primary antibody (1:1000) and imaged using the Pico Chemiluminescent Substrate (ThermoFisher) and a Kodak X-Omat film processor. No increase in ERK1/2 phosphorylation was observed in response to rBsg treatment, even at the 5min and 10min time periods.

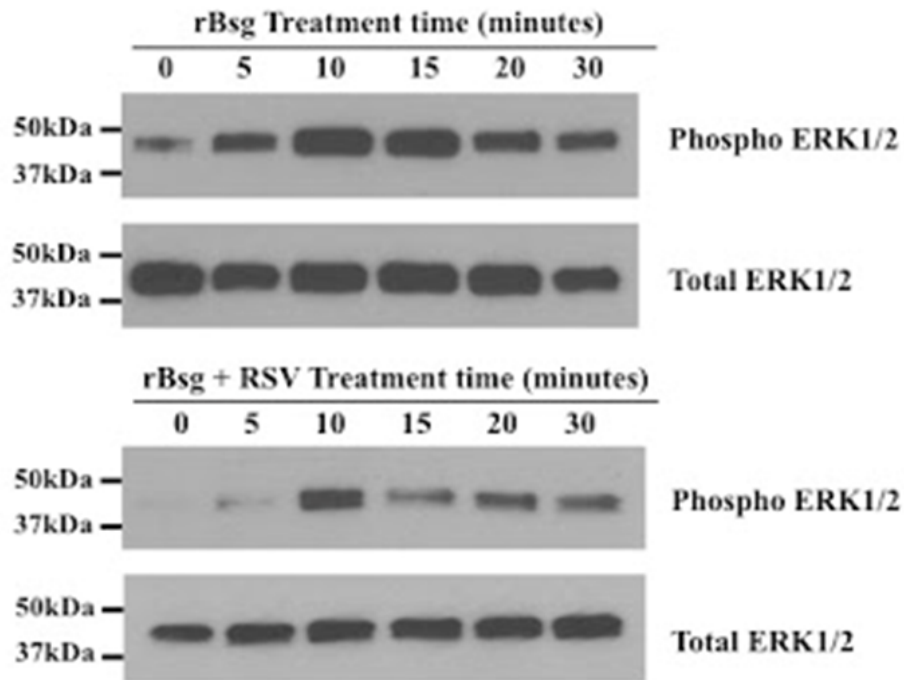


Figure 22. Revised immunoblot analysis of U87MG cells treated with rBsg or rBsg+30 μ M RSV. For this assay, the time course was modified to include longer treatment times at 37°C. U87MG human GBM cells were treated either 10 μ g/mL rBsg only or 10 μ g/mL rBsg+30 μ M RSV as a pre-treatment and a co-treatment in serum-free culture media for the indicated time period at 37°C. Cells were then lysed and the protein fraction was collected and subjected to Western blot analysis. Immunoblotting was performed using the anti-phosphoERK1/2 primary antibody (1:2000) and the anti-ERK1/2 primary antibody (1:1000) and imaged using the Pico Chemiluminescent Substrate (ThermoFisher) and a Kodak X-Omat film processor. These images were taken after a 30sec exposure to the film. The blots revealed that rBsg stimulates a transient increase in ERK1/2 phosphorylation, peaking between 10min and 15min, and that the rBsg-mediated phosphorylation is reduced by the presence of Resveratrol.

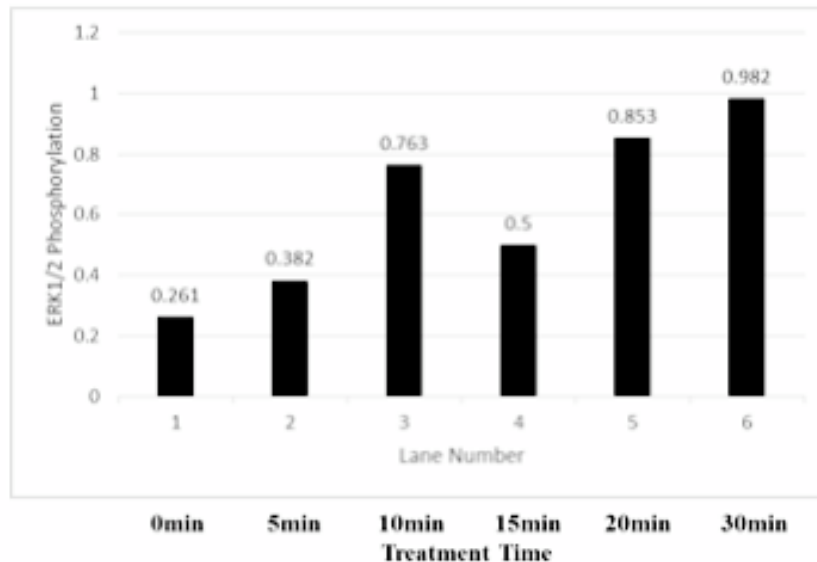


Figure 23. Resveratrol treatment of U87MG cells reduces peak rBsg-induced ERK1/2 phosphorylation at body temperature (37 °C). U87MG cells were treated with either media containing 30µg/mL rBsg alone or 30µg/mL rBsg+30µM RSV for the listed time periods prior to lysis. Lysates were probed for ERK1/2 activation to determine the degree of inhibition by RSV. The values listed represent the amount of ERK1/2 phosphorylation seen in cells treated with RSV and rBsg compared to cells given only rBsg at the same time period. The peak phosphorylation event seen in rBsg-only treated cells at 10mins is reduced by 24.7%. After the 15min time point, the degree of RSV-mediated ERK1/2 inhibition decreases and ERK1/2 phosphorylation levels begin to closely resemble the rBsg-only treated cells at the same treatment time. These results indicate that the degree of ERK1/2 inhibition in response to rBsg is not as large as RSV inhibition of FBS serum-stimulated ERK1/2 activation.

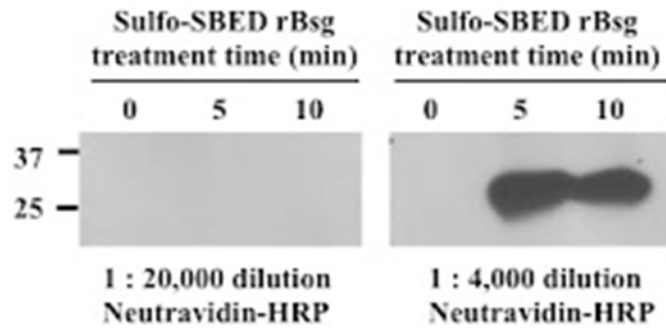


Figure 24. NeutrAvidin-HRP Blot for Putative Receptors of rBsg-SBED Bait Protein. U87MG cells were serum starved before being treated with 30µg per milliliter of SBED-labeled rBsg protein in serum free media for the indicated time period at 37°C. The 10cm plates containing the treated cells were crosslinked with UV light in a Stratalinker (Stratagene) at a distance of 5cm for 5 minutes at maximum power. The media was removed and the cells lysed and processed for immunoblotting using NeutrAvidin-HRP (ThermoScientific) at two different dilutions: 1:20,000 (*Left*) and 1:4,000 (*Right*). The 1:20,000 was the greatest dilution suggested by the Sulfo-SBED manufacturer (ThermoScientific). The 1:4,000 dilution revealed a single band at approximately the molecular weight of the rBSG protein, suggesting the lack of label transfer from the recombinant protein to potential cell surface receptor proteins.

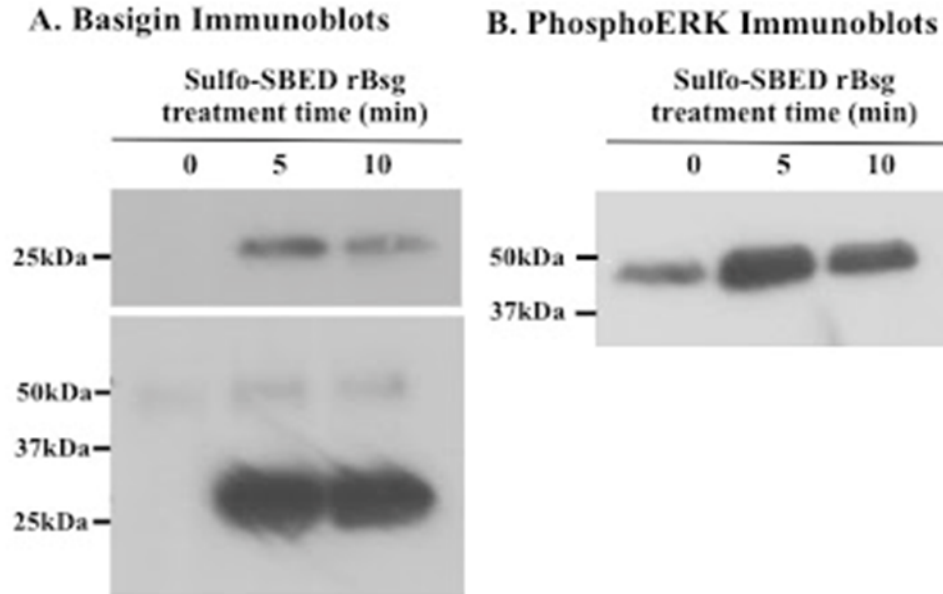


Figure 25. Evidence for rBsg-ECD labeling of U87MG cells and the activation of the ERK1/2 signaling pathway. U87-MG cells were treated with 30 μ g/mL rBsg-SBED protein in serum free media for the indicated time period at 37°C before being crosslinked with a UV Stratalinker (Stratagene) at a distance of 5cm for 5mins at maximum power, making the total exposure times 10 and 15min, respectively. The cells were washed, lysed and the lysates were immunoblotted for human basigin and phosphorylated ERK1/2. *A*) Immunoblotting with the anti-human EMMPRIN-ECD monoclonal antibody (1:1000) and goat anti-mouse HRP-conjugated secondary antibody (1:25000). Top: A short exposure identified only the rBsg-SBED protein at ~25kDa. Bottom: A longer exposure revealed the at roughly 26kDa, as well as the endogenous Bsg-2 protein at ~50kDa This image was obtained after a 5min exposure to film before preprocessing. *B*) Immunoblotting with the anti-phosphoERK1/2 primary antibody (1:2000) and goat anti-rabbit HRP-conjugated secondary antibody (1:25000). In this experiment, maximal ERK1/2 phosphorylation occurred after a 5 minute treatment with the rBsg-SBED protein at 37°C and 5 minutes of exposure to UV light at room temperature (10 minutes total time).

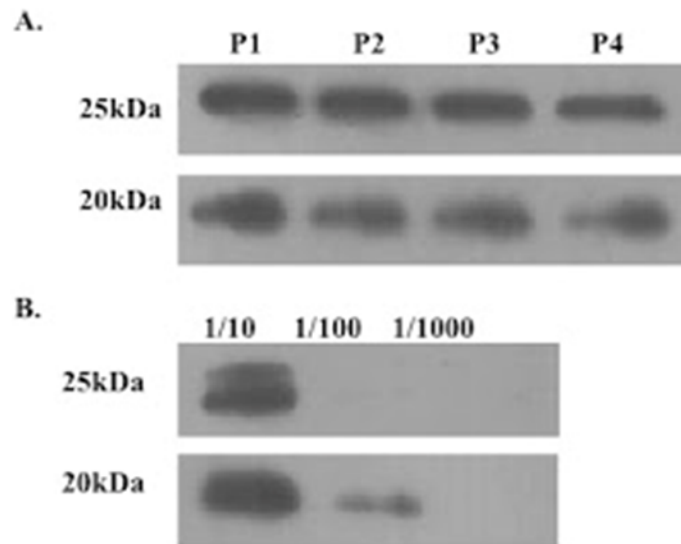


Figure 26. Second Attempt of NeutrAvidin-HRP Blots for Putative Receptors of rBsg-SBED bait protein. *A*) Four identical plates (P1-P4) of U87-MG cells were treated with 120µg/mL rBsg-SBED, 4x the original treatment of 30µg/mL rBsg-SBED, in serum-free EMEM for 5mins at 37C before being exposed to UV light in a UV Stratalinker (Stratagene) at a distance of 5cm for 5mins at maximum power. Cells were lysed and the lysates were run onto gels under either denaturing (*top*) or non-denaturing conditions (*bottom*) and were probed for the presence of biotinylated proteins using NeutrAvidin-HRP (ThermoScientific) (1:4000). Non-denatured samples moved farther down the gel than their denatured counterparts. Only rBsg-SBED was identified in the samples. *B*) Serial dilutions of stock rBsg-SBED were made and run out under denaturing (*top*) or non-denaturing conditions (*bottom*) to test for issues with biotin tag cleavage from the rBsg-SBED proteins. Presence of biotinylated proteins is expected in the non-denatured samples, whereas the presence of biotinylated rBsg-SBED in the 1/10 was not expected, given that the biotin tags should have been cleaved off when exposed to DTT in the SDS-PAGE sample buffer. The images were obtained after a 30sec exposure to film. The blots were imaged using the West Pico chemiluminescent substrate (ThermoScientific) and a Kodak X-Omat film processor.

DISCUSSION

Glioblastoma multiforme (GBM) is the most common malignant form of human brain cancer. GBMs are comprised of supportive cells within the brain called glial cells that tend to be astrocytes. These tumors are characterized by the presence of necrotic tissue, a grim prognosis for patients, and their highly aggressive nature. Basigin-2 (Bsg-2) is a transmembrane glycoprotein commonly found in healthy lymphocytes, endothelial cells, and retinal cells, and is implicated in spermatogenesis, tissue remodeling, and embryonic implantation. In cancerous cells, Bsg is highly upregulated at the cell surface where it is released by vesicular shedding into the ECM^{1, 14-18}. In a cancerous environment, and normal tissues as well, Bsg-2 mediates the production of matrix metalloproteinases (MMPs) from stromal and cancer cells. These MMPs degrade the extracellular matrix, providing an environment favorable to metastasis and tumor growth. Bsg has been confirmed to bind to itself at the cell surface of normal human endothelial cells, given its nature of homodimerization, by the use of a recombinant form of Bsg-2 (rBsg)¹. Binding of rBsg was shown to induce the activation of the MAPK signaling pathway, observed through the activation of ERK1/2, a protein implemented in cell survival and cell cycle progression. This relationship has not been observed in a GBM model. This project sought to establish the presence of rBsg-Bsg-2 binding at the surface

of GBM cells that would contribute to the activation of the MAPK pathway and illuminate a pro-survival autocrine/juxtacrine signaling loop between GBM tumor cells.

In order to confirm the hypothesis of this project, rBsg had to be generated for use in experimentation. rBsg is a ~25kDa protein consisting of the extracellular domain of the human basigin-2 protein that mimics the biologically active, highly glycosylated form of Bsg^{1, 11, 12}. Transformed *E. coli* bacteria needed to be grown and induced to express the rBsg in the periplasmic space, where the protein would retain the two disulfide bridges present between the Ig-folds of the protein. Once the bacteria were submitted to osmotic shock lysis, the protein could be purified through the use of cobalt beads that bound the histidine tag on the rBsg. SDS-PAGE and Western blot analysis revealed that rBsg had been successfully produced and purified. Although the banding on the Western blot is altered due to shifting of the gel just prior to the transfer to PVDF membrane. There were also issues in getting enough protein isolated for use in the experiment. In previous attempts by Belton et al. (2008), rBsg concentrations after purification reached into multiple milligrams levels, whereas isolations for this work totaled 0.6873mg. It has been theorized that the protein induction conditions weren't correct. In future attempts, the induction should go longer in a 37°C environment to provide optimal time and functional conditions for the *E. coli* bacteria used.

Resveratrol was selected to serve as the inhibitor to ERK1/2 based on previous work by Huang et al. (2008)⁵³. RSV is a phytoalexin plant polyphenol commonly found in grapes, berries, and the bark of some species of pine tree. It is unclear exactly how RSV inhibits ERK1/2 phosphorylation, but it is known that the molecule is an antagonist of EGFR-dependent ERK1/2 activation and that it is endocytosed at lipid rafts, where the

EGFR protein is located^{58, 59}. Taken together, RSV may inhibit ERK1/2 by modulation of the EGFR-dependent MAPK signaling cascade at lipid rafts on cells, but that is only speculation. In order to determine what method of treatment should be employed when using the RSV, an assay was constructed to test the effects of pre-treatments of RSV in serum-free media prior to treatment of U87-MG cells with conditioned media and the effects of a co-treatment of conditioned media in the presence of RSV. Western blot analysis for phosphorylated ERK1/2 levels indicated that the most effective ERK1/2 inhibition was observed when U87-MG cells were pre-treated with 30 μ M RSV and co-treated with conditioned media in the presence of 30 μ M RSV. The purpose of having a pre-treatment of 2hrs in conjunction with the co-treatment was to ensure that any inhibitor effects weren't interrupted. These cells were treated at room temperature, while later cell treatments were done at 37°C. Although the temperature difference may have had an effect on the treatment, it was deemed acceptable to use these results as evidence the selected method of RSV treatment of a pre- and co-treatment. High levels of ERK1/2 phosphorylation seen in unstimulated cells is most likely due to the fact that the cells were washed with PBS prior to treatment and prior to lysis with 1% NP-40 buffer. The cold PBS used to wash the cells cold-shocked the cells, causing a change in the intracellular landscape. In later blots where washes were eliminated, unstimulated cells exhibited almost no levels of ERK1/2 phosphorylation. However, there is still expected to have some level of constitutively activated ERK1/2, given the transformed nature of cancer cells. This can be attributed, possibly, to the presence of EGFRvIII. This form of the EGFR receptor is truncated, missing the extracellular domain, and is constitutively activated.

Early control cell Western blots exhibited numerous issues that shed light on errors in the protocol designed from them. Initial problems were speculated to be due to faulty antibodies. However, it was determined that smearing of bands and improper labeling were due to the use of improper antibody dilution buffers that inhibited proper binding of the antibodies to their target proteins. This was addressed by following manufacturer protocols and results improved. There were other factors that could have affected the quality of the images obtained, including improper handling of the PVDF membrane prior to the transfer step of the Western blot. Eventually, all mistakes were corrected, leading to clearer blot images.

Control U87-MG cells were needed in order to compare the phosphorylation of ERK1/2 induced by normal growth factors and nutrients to any that might be seen by the rBsg protein to be used later. U87-MG cells were treated with 1mL warmed 10% FBS in EMEM for two different time courses. The initial time course consisted of incubations with treatment media at room temperature, washes of cells with PBS, and time periods of 0sec, 30sec, 1min, 2min, 5min, and 10min. The Western blots of these cell lysates did reveal that as time progressed, ERK1/2 phosphorylation increased up to the 10min time point. The high amount of phosphorylated ERK1/2 seen in the 0sec time point, which are cells that have gone unstimulated, can be most likely be attributed to the addition of cold PBS to wash the cells both before and after treatments. This caused the cells to be cold-shocked, inducing changes in the cells that don't accurately reflect what happens to the cells upon addition of the treatment media at any time point, let alone the 0sec time point. Due to this, PBS washes were eliminated from the protocol. In cells treated with serum-containing media with RSV, a high amount of ERK1/2 inhibition can be observed. The

darker bands at the later time points could indicate that the RSV eventually wears off. However, because of the cold-shock of these cells, the images were deemed unreliable for determination of RSV's effect on serum-stimulated ERK1/2 activation.

Initial rBsg treatments used the same time course as the initial control cells described earlier, albeit without PBS washes. The treatments still occurred for time periods of 0sec, 30sec, 1min, 2min, 5min, and 10min at room temperature. rBsg protein was given to cells in 1mL serum-free EMEM at a concentration of 10 μ g/mL with or without 30 μ M RSV pre- and co-treatment. The removal of PBS washes did, in fact, decrease the amount of phosphorylated ERK1/2 seen in the unstimulated cells. However, the blot showed consistent levels of ERK1/2 phosphorylation across all time points, indicating that the rBsg wasn't having any effect on ERK1/2 activation. The same could be said about the cells treated with rBsg and RSV. While the baseline levels of pERK1/2 were decreased in RSV-treated cells, there were no other trends observed. The lack of ERK1/2 activation is most likely due to the fact that the plates were incubated at room temperature. In order for Bsg, or rBsg, to have any effect, the protein needs to bind to the cell and be endocytosed. There should be a small degree of ERK1/2 activation under the right conditions at the 5min time point that was not seen, suggesting that endocytosis of rBsg did not occur. The shorter time periods used for these cell treatments also fail to give a clear picture of what happens after the 10min time point. Since it can take some amount of time for any affect to be observed, at a 10min cutoff would exclude any potential effects that occurs after that relatively short time point. This prompted a change to a longer time course, similar to the one used by Belton et al. (2008), that would be

incubated at 37°C¹. This ensured that the plates of cells could be transferred to/from the 37°C incubator, treated, aspirated, and lysed in a timely fashion.

New control cells needed to be grown, treated, and lysed under the same conditions as the next rBsg cells. U87-MG cells were treated with 2mL serum-containing media with or without a RSV pre- and co-treatment for time periods of 0min, 5min, 10min, 15min, 20min, and 30min at 37°C. The addition of an extra milliliter of media was to ensure that the cells were completely covered by media. In the images obtained, pERK1/2 levels increased up until the 10min point where they peak, drop off slightly, and then hold steady, with almost no pERK1/2 present in the unstimulated 0min time point cells. This is in stark contrast to the initial control cells collected, providing a much clearer image of what happens when cells are given the growth factors and nutrients expected to induce cell cycle progression and growth. The RSV-treated control cells exhibited highly altered ERK1/2 phosphorylation when compared to the cells not treated with RSV. The peak phosphorylation event seen at the 10min time point seen in the non-inhibited cells is decreased by 49.8% in the cells treated with RSV (Fig. 20). However, the effects of the RSV appear to wear off, evidenced by the dark band in the 30min time point cells. This could be due to endocytosis at lipid rafts, where the EGFR receptor is located, which would eventually deplete the amount of usable RSV, however this is just speculation. The phosphorylation seen in U87-MG cells when exposed to normal nutrients and growth factors establishes the control that will be used to compare to the effects of rBsg protein exposure.

U87-MG cells were ready to be treated with rBsg grown during the purification steps, this time, for the longer time course and incubation temperature of 37°C and with

2mL of conditioned media. Cells were given either serum-free EMEM with 10µg/mL rBsg or 10µg/mL rBsg+30µM RSV for the established time course. Western blot analysis revealed an increase in ERK1/2 phosphorylation in response to the treatment with rBsg. There was a peak phosphorylation event between the 10 and 15min time points that decreased at the later time points. This is in contrast to the constant plateau seen in the control cells stimulated with serum. Signaling activation is due to the endocytosis of the rBsg into the cells. This interaction indicates that uptake of Bsg proteins on vesicles will cause the activation of the MAPK pathway, even in the absence of growth factors and nutrients. This is reminiscent of the tumor microenvironment where an overabundance of cells growing and proliferating depletes the availability of the growth factors and nutrients necessary for signaling growth. The MAPK pathway activation, signaled by increased levels of phosphorylated ERK1/2 mediated by exposing the cells to rBsg, indicates that an autocrine/juxtacrine loop exists that allows cells to continue to grow in the absence of growth factors, proving half of the hypothesis correct. Interestingly, RSV inhibited the rBsg-mediated ERK1/2 phosphorylation by 23.7% (Fig. 23). There was no increase in phosphorylation at the later time periods. This inhibition indicates that the method of inhibition must be the same between cells given serum and cells given the rBsg protein. Fetal bovine serum used in cell culture media is known to act through the EGFR-Ras-MAPK pathway described earlier. The EGFR receptor and Bsg-2 are located in close proximity to each other in lipid rafts. Since it's been established that treatment of GBM cells with rBsg stimulates ERK1/2 phosphorylation, and that ERK1/2 phosphorylation also occurs through EGFR signaling, it could be possible that both EGFR and Bsg-2 work in conjunction to transmit signals to the inside of the cells. This is

evidenced by the fact that RSV abrogated both serum-stimulated and rBsg-stimulated ERK1/2 phosphorylation. With that revelation, if rBsg is indeed acting through a Bsg-2/EGFR cooperation, it opens the door for combination treatments that target both receptors rather than just one at a time, or drugs that act on more than one pro-cancerous pathway, meaning better outlooks for patients diagnosed with GBM. RSV could potentially be one of these treatment molecules. The inhibition of both EGFR signaling and Bsg-2 via RSV could have more potent effects than targeting one or the other. It is also possible that RSV acts on not just the EGFR and Bsg-2 receptors, but also on the downstream effectors as well.

In order to firmly establish a mechanism for rBsg stimulation of U87-MG cells, rBsg protein gifted to me by Dr. Robert Belton was labeled with the Sulfo-SBED heterotrifunctional UV light-activated cross-linker (ThermoFisher) with a biotin tag. When rBsg is attached to the Sulfo-SBED reagent, the rBsg should bind to a putative receptor. When activated with UV light, the SBED reagent attached to the rBsg should transfer the biotin tag to anything bound to the rBsg protein. The tag can then be cleaved from the rBsg via denaturation during SDS-PAGE analysis, leaving the tag on the putative receptor, and then imaged using NeutrAvidin-HRP protein after a Western blot. The results of the initial label transfer trial indicate that no label transfer occurred, evidenced by the presence of only biotinylated rBsg protein in lysate samples, most likely caused by dimerization of rBsg-SBED molecules in solution. It was initially believed that there wasn't enough protein in solution to overcome any self-dimerization and have an appreciable label transfer occur, leading to the decision to try 120 μ g/mL rBsg-SBED treatments. The potential issue of inadequate denaturation and thus, cleavage of the biotin

from the rBsg, was addressed by running lysate samples under both denaturing and nondenaturing conditions along with serial dilutions of the rBsg-SBED. The results indicated no difference from the initial experiment, supported by the presence of only biotinylated rBsg in lysate samples. The serial dilutions indicated that in denaturing conditions, some biotinylated rBsg molecules exist in the 1/10 dilution only. The nondenatured serial dilution samples showed the presence of more biotinylated rBsg in the 1/10 and 1/100 dilutions, while none was observed in the 1/1000 dilution. This is most likely due to the limitations of the ECL detection system. Even though there wasn't a label transfer, U87-MG cells treated with rBsg-SBED showed high increases in ERK1/2 phosphorylation after treatment. This indicates that the protein is indeed binding to the cell surface and causing a stimulus, supporting the initial experiments where cells were treated with pure rBsg protein. This activation was observed in a similar fashion, peaking at 10mins post-exposure. There is also phosphorylated ERK1/2 in the lysates not treated with rBsg-SBED. This can most likely be attributed to the 5min exposure to UV light that took place as the cells try to fight the effects of the UV radiation. Despite the lack of evidence supporting my hypothesis that rBsg stimulates ERK1/2 via Bsg-2, it is likely that this is only due to issues with the label transfer and not with the actual binding to the receptor. In the work by Belton et al. (2008), Bsg-2 will bind rBsg at the surface of human endometrial stromal cells. Based on this finding, rBsg should bind to Bsg-2 at the surface of GBM cells, given the fact that Bsg-2 is highly upregulated on their surfaces. This notion is supported by Bsg-2's ability to homodimerize, a characteristic shared by rBsg. Given the presence of biotinylated rBsg proteins alone in the label transfer experiments, it's likely that the rBsg proteins formed homodimers and transferred their

biotin tags to each other. Belton et al. (2008) also illustrated that rBsg also bound to other receptors that weren't identified. As stated earlier, one of these receptors is most likely EGFR, given the fact that it was shown that RSV blocked ERK1/2 phosphorylation in response to treatment with only rBsg, proving at least half of the hypothesis correct. This points to a cooperation between EGFR and Bsg-2 and potentially other receptors found in the lipid rafts of cells, where these proteins are found. However, due to lack of evidence, this relationship will have to be investigated in future work.

CONCLUSION

Taken together, the results of this project highlight an existing means for the activation of the ERK1/2 pathway mediated by solubilized Bsg-2 proteins, mimicking those released by cancerous cells to affect the surrounding tumor environment. The activation of ERK1/2 caused by exposure of human GBM cells to rBsg protein, both attached to the SBED reagent and pure, indicate that somehow, the protein is being taken up by cells. The purpose of the SBED label transfer was to identify the potential receptors for the protein, but the experiment revealed inconclusive results. More likely than not, the rBsg is binding to Bsg-2 at the cell surface, as evidenced in the work by Belton et al. (2008) and the use of the rBsg protein, developed by their work, in this research. Resveratrol, when given to cells at the same time as the rBsg or FBS, caused an inhibition of ERK1/2 phosphorylation. This indicates that the two treatments, rBsg and FBS, operate under a similar mechanism. Given the fact that RSV affects EGFR-mediated ERK1/2 activation, this could mean that the ERK1/2 signaling activation is mediated by the rBsg at the EGFR in lipid rafts, where normal Bsg-2 is also located. Future experiments should aim to establish a connection between the rBsg protein, Bsg-2, and the EGFR receptor.

WORKS CITED

1. Belton, Robert J. et al. "Basigin-2 Is a Cell Surface Receptor for Soluble Basigin Ligand." *Journal of Biological Chemistry* 283.26 (2008): 17805–17814. www.jbc.org. Web.
2. Young, Richard M. et al. "Current Trends in the Surgical Management and Treatment of Adult Glioblastoma." *Annals of Translational Medicine* 3.9 (2015): n. pg. *PubMed Central*. Web. 18 Feb. 2017.
3. "World Health Organization, World Cancer Report 2014." *SEARO*. N.p., n.d. Web. 7 Mar. 2017.
4. Huang, Huiyong et al. "Resveratrol Reverses Temozolomide Resistance by Downregulation of MGMT in T98G Glioblastoma Cells by the NF- κ B-Dependent Pathway." *Oncology reports* 27.6 (2012): 2050. Print.
5. Hayden, Erika Check. "Genomics Boosts Brain-Cancer Work." *Nature News* 463.7279 (2010): 278–278. www.nature.com. Web.
6. Montano, Nicola et al. "Expression of EGFRvIII in Glioblastoma: Prognostic Significance Revisited." *Neoplasia (New York, N.Y.)* 13.12 (2011): 1113–1121. Print.
7. Nyati, Mukesh K. et al. "Integration of EGFR Inhibitors with Radiochemotherapy." *Nature Reviews Cancer* 6.11 (2006): 876–885. www.nature.com. Web.
8. Chen, Li et al. "Expression of Basigin in Reproductive Tissues of Estrogen Receptor- α or - β Null Mice." *Reproduction* 139.6 (2010): 1057–1066. www.reproduction-online.org. Web.
9. "BSG - Basigin Precursor - Homo Sapiens (Human) - BSG Gene & Protein." N.p., n.d. Web. 26 June 2017.
10. Weidle, Ulrich H. et al. "Cancer-Related Issues of CD147." *Cancer Genomics-Proteomics* 7.3 (2010): 157–169. Print.
11. Huang, Wan et al. "Modulation of CD147-Induced Matrix Metalloproteinase Activity: Role of CD147 N-Glycosylation." *Biochemical Journal* 449.2 (2013): 437–448. www.biochemj.org. Web.
12. Tang, Wei, Sharon B. Chang, and Martin E. Hemler. "Links between CD147 Function, Glycosylation, and Caveolin-1." *Molecular Biology of the Cell* 15.9 (2004): 4043–4050. *PubMed*. Web.
13. Curtin, Kathryn D., Ian A. Meinertzhagen, and Robert J. Wyman. "Basigin (EMMPRIN/CD147) Interacts with Integrin to Affect Cellular Architecture." *Journal of Cell Science* 118.12 (2005): 2649–2660. jcs.biologists.org. Web.
14. Gabison, Eric E. et al. "EMMPRIN/CD147, an MMP Modulator in Cancer,

- Development and Tissue Repair.” *Biochimie* 87.3–4 (2005): 361–368. *ScienceDirect*. Web.
15. Liotta, L.A., Kohn, E.C.. “The Microenvironment of the Tumor-Host Interface.” *Nature* 411.6835 (2001): 375–9. Web.
 16. Huet, Eric, Eric E. Gabison, et al. “Role of Emmprin/CD147 in Tissue Remodeling.” *Connective Tissue Research* 49.3–4 (2008): 175–179. *Taylor and Francis+NEJM*. Web.
 17. Huet, Eric, Benoit Vallée, et al. “EMMPRIN Modulates Epithelial Barrier Function through a MMP–Mediated Occludin Cleavage.” *The American Journal of Pathology* 179.3 (2011): 1278–1286. *PubMed Central*. Web.
 18. Kanekura, Takuro, and Xiang Chen. “CD147/Basigin Promotes Progression of Malignant Melanoma and Other Cancers.” *Journal of Dermatological Science* 57.3 (2010): 149–154. *ScienceDirect*. Web.
 19. Biswas, Chitra et al. “The Human Tumor Cell-Derived Collagenase Stimulatory Factor (Renamed EMMPRIN) Is a Member of the Immunoglobulin Superfamily.” *Cancer Research* 55.2 (1995): 434–439. Print.
 20. Biswas, Chitra. “Collagenase Stimulation in Cocultures of Human Fibroblasts and Human Tumor Cells.” *Cancer Letters* 24.2 (1984): 201–207. *ScienceDirect*. Web.
 21. Grass, G. Daniel et al. “CD147, CD44, and the Epidermal Growth Factor Receptor (EGFR) Signaling Pathway Cooperate to Regulate Breast Epithelial Cell Invasiveness.” *Journal of Biological Chemistry* 288.36 (2013): 26089–26104. www.jbc.org. Web.
 22. Yan, Li, Stanley Zucker, and Bryan P. Toole. “Roles of the Multifunctional Glycoprotein, Emmprin (Basigin; CD147), in Tumour Progression.” *Thrombosis and Haemostasis* (2005): n. pag. *CrossRef*. Web. 9 Sept. 2015.
 23. Yang, Min et al. “Prognostic Significance of CD147 in Patients with Glioblastoma.” *Journal of Neuro-Oncology* 115.1 (2013): 19–26. link.springer.com. Web.
 24. Liang, Qinchuan et al. “Inhibition of Basigin Expression in Glioblastoma Cell Line via Antisense RNA Reduces Tumor Cell Invasion and Angiogenesis.” *Cancer Biology & Therapy* 4.7 (2005): 759–762. *Taylor and Francis+NEJM*. Web.
 25. Sameshima, Tetsuro et al. “Expression of Emmprin (CD147), a Cell Surface Inducer of Matrix Metalloproteinases, in Normal Human Brain and Gliomas.” *International Journal of Cancer* 88.1 (2000): 21–27. *Wiley Online Library*. Web.
 26. Reed, Bruce H. et al. “Integrin-Dependent Apposition of Drosophila Extraembryonic Membranes Promotes Morphogenesis and Prevents Anoikis.” *Current biology: CB* 14.5 (2004): 372–380. *PubMed*. Web.
 27. Dai, Jing-yao et al. “The Interaction of HAb18G/CD147 with Integrin alpha6beta1 and Its Implications for the Invasion Potential of Human Hepatoma Cells.” *BMC Cancer* 9 (2009): 337. *PubMed*. Web.
 28. Lathia, Justin D. et al. “Integrin Alpha 6 Regulates Glioblastoma Stem Cells.” *Cell stem cell* 6.5 (2010): 421–432. *PubMed Central*. Web.
 29. Chintala, S. K. et al. “Modulation of Matrix Metalloprotease-2 and Invasion in Human Glioma Cells by Alpha 3 Beta 1 Integrin.” *Cancer Letters* 103.2 (1996): 201–208. Print.

30. Chen, Yanke et al. "Upregulation of HAb18G/CD147 in Activated Human Umbilical Vein Endothelial Cells Enhances the Angiogenesis." *Cancer Letters* 278.1 (2009): 113–121.
31. Voigt, Heike et al. "CD147 Impacts Angiogenesis and Metastasis Formation." *Cancer Investigation* 27.3 (2009): 329–333. *PubMed*. Web.
32. Munaut, Carine et al. "Vascular Endothelial Growth Factor Expression Correlates with Matrix Metalloproteinases MT1-MMP, MMP-2 and MMP-9 in Human Glioblastomas." *International Journal of Cancer* 106.6 (2003): 848–855. *Wiley Online Library*. Web.
33. Yin, Haoyuan, Ying Shao, and Xuan Chen. "The Effects of CD147 on the Cell Proliferation, Apoptosis, Invasion, and Angiogenesis in Glioma." *Neurological Sciences* 38.1 (2017): 129–136. *link.springer.com*. Web.
34. Heiden, Matthew G. Vander, Lewis C. Cantley, and Craig B. Thompson. "Understanding the Warburg Effect: The Metabolic Requirements of Cell Proliferation." *Science* 324.5930 (2009): 1029–1033. *science.sciencemag.org*. Web.
35. Fais, S. "Proton Pump Inhibitor-Induced Tumour Cell Death by Inhibition of a Detoxification Mechanism." *Journal of Internal Medicine* 267.5 (2010): 515–525. *Wiley Online Library*. Web.
36. Miranda-Gonçalves, Vera et al. "Hypoxia-Mediated Upregulation of MCT1 Expression Supports the Glycolytic Phenotype of Glioblastomas." *Oncotarget* 7.29 (2016): 46335–46353. *www.impactjournals.com*. Web.
37. Halestrap, Andrew P., and Nigel T. Price. "The Proton-Linked Monocarboxylate Transporter (MCT) Family: Structure, Function and Regulation." *Biochemical Journal* 343.2 (1999): 281–299. *www.biochemj.org*. Web.
38. Halestrap, Andrew P. "The Monocarboxylate Transporter Family--Structure and Functional Characterization." *IUBMB life* 64.1 (2012): 1–9. *PubMed*. Web.
39. Marchiq, Ibtissam et al. "Genetic Disruption of Lactate/H⁺ Symporters (MCTs) and Their Subunit CD147/BASIGIN Sensitizes Glycolytic Tumor Cells to Phenformin." *Cancer Research* 75.1 (2015): 171–180. *PubMed*. Web.
40. Philp, Nancy J. et al. "Loss of MCT1, MCT3, and MCT4 Expression in the Retinal Pigment Epithelium and Neural Retina of the 5A11/Basigin-Null Mouse." *Investigative Ophthalmology & Visual Science* 44.3 (2003): 1305–1311. Print.
41. Baba, Miyako et al. "Blocking CD147 Induces Cell Death in Cancer Cells through Impairment of Glycolytic Energy Metabolism." *Biochemical and Biophysical Research*
42. Yurchenko, V. et al. "CD147 Is a Signaling Receptor for Cyclophilin B." *Biochemical and Biophysical Research Communications* 288.4 (2001): 786–788. *PubMed*. Web.
43. Li, Min et al. "Cyclophilin A Is Overexpressed in Human Pancreatic Cancer Cells and Stimulates Cell Proliferation through CD147." *Cancer* 106.10 (2006): 2284–2294. *Wiley Online Library*. Web.
44. Najyb, Ouafa, Louise Brissette, and Eric Rassart. "Apolipoprotein D Internalization Is a Basigin-Dependent Mechanism." *Journal of Biological Chemistry* 290.26 (2015): 16077–16087. *www.jbc.org*. Web.
45. Nabeshima, Kazuki et al. "Emmprin (Basigin/CD147): Matrix Metalloproteinase

- Modulator and Multifunctional Cell Recognition Molecule That Plays a Critical Role in Cancer Progression.” *Pathology International* 56.7 (2006): 359–367. *Wiley Online Library*. Web.
46. Roskoski, Robert. “ERK1/2 MAP Kinases: Structure, Function, and Regulation.” *Pharmacological Research* 66.2 (2012): 105–143. *PubMed*. Web
 47. Meloche, S., and J. Pouyssegur. “The ERK1/2 Mitogen-Activated Protein Kinase Pathway as a Master Regulator of the G1- to S-Phase Transition.” *Oncogene* 26.22 (2007): 3227–3239. *www.nature.com*. Web.
 48. Mebratu, Yohannes, and Yohannes Tesfaigzi. “How ERK1/2 Activation Controls Cell Proliferation and Cell Death: Is Subcellular Localization the Answer?” *Cell Cycle* 8.8 (2009): 1168–1175. *Taylor and Francis+NEJM*. Web.
 49. Balmanno, K., and S. J. Cook. “Tumour Cell Survival Signalling by the ERK1/2 Pathway.” *Cell Death and Differentiation* 16.3 (2009): 368–377. *PubMed*. Web.
 50. Xia, Wenle et al. “Anti-Tumor Activity of GW572016: A Dual Tyrosine Kinase Inhibitor Blocks EGF Activation of EGFR/erbB2 and Downstream Erk1/2 and AKT Pathways.” *Oncogene* 21.41 (2002): 6255–6263. *CrossRef*. Web.
 51. Tomé-Carneiro, Joao et al. “Resveratrol and Clinical Trials: The Crossroad from In Vitro Studies to Human Evidence.” *Current Pharmaceutical Design* 19.34 (2013): 6064–6093. *PubMed Central*. Web.
 52. Lagouge, Marie et al. “Resveratrol Improves Mitochondrial Function and Protects against Metabolic Disease by Activating SIRT1 and PGC-1 α .” *Cell* 127.6 (2006): 1109– 1122. *www.cell.com*. Web.
 53. Huang, Zhouqing et al. “Resveratrol Inhibits EMMPRIN Expression via P38 and ERK1/2 Pathways in PMA-Induced THP-1 Cells.” *Biochemical and Biophysical Research Communications* 374.3 (2008): 517–521. *ScienceDirect*. Web.
 54. Athar, Mohammad et al. “Multiple Molecular Targets of Resveratrol: Anti-Carcinogenic Mechanisms.” *Archives of Biochemistry and Biophysics* 486.2 (2009): 95–102. *ScienceDirect*. Web.
 55. Mustafi, Soumyajit Banerjee, Prabir K. Chakraborty, and Sanghamitra Raha. “Modulation of Akt and ERK1/2 Pathways by Resveratrol in Chronic Myelogenous Leukemia (CML) Cells Results in the Downregulation of Hsp70.” *PLOS ONE* 5.1 (2010): e8719. *PLoS Journals*. Web.
 56. Ahmad, Nihal et al. “Resveratrol Causes WAF-1/p21-Mediated G1-Phase Arrest of Cell Cycle and Induction of Apoptosis in Human Epidermoid Carcinoma A431 Cells.” *Clinical Cancer Research* 7.5 (2001): 1466–1473. Print.
 57. Colin, Didier et al. “Endocytosis of Resveratrol via Lipid Rafts and Activation of Downstream Signaling Pathways in Cancer Cells.” *Cancer Prevention Research* 4.7 (2011): 1095–1106. *cancerpreventionresearch.aacrjournals.org*. Web.
 58. Stewart, Jubilee R., and Catherine A. O’Brian. “Resveratrol Antagonizes EGFR-Dependent Erk1/2 Activation in Human Androgen-Independent Prostate Cancer Cells with Associated Isozyme-Selective PKC Alpha Inhibition.” *Investigational New Drugs* 22.2 (2004): 107–117. *PubMed*. Web.
 59. Donnelly, Louise E. et al. “Anti-Inflammatory Effects of Resveratrol in Lung Epithelial Cells: Molecular Mechanisms.” *American Journal of Physiology - Lung Cellular and Molecular Physiology* 287.4 (2004): L774–L783.

ajplung.physiology.org. Web

60. Xiong, Wei et al. "Resveratrol Suppresses Human Glioblastoma Cell Migration and Invasion via Activation of RhoA/ROCK Signaling Pathway." *Oncology Letters* 11.1 (2016): 484–490. *PubMed Central*. Web.
61. Yang, Yi-Ping et al. "Resveratrol Suppresses Tumorigenicity and Enhances Radiosensitivity in Primary Glioblastoma Tumor Initiating Cells by Inhibiting the STAT3 Axis." *Journal of cellular physiology* 227.3 (2012): 976–993. Print.

APPENDIX A

License to use Figure 2 from “Integration of EGFR inhibitors with radiochemotherapy” by Nyati et al. received from Nature Publishing Group.

License Number	4143291113978
License date	Jul 06, 2017
Licensed Content Publisher	Nature Publishing Group
Licensed Content Publication	Nature Reviews Cancer
Licensed Content Title	Integration of EGFR inhibitors with radiochemotherapy
Licensed Content Author	Mukesh K. Nyati, Meredith A. Morgan, Felix Y. Feng and Theodore S. Lawrence
Licensed Content Date	Oct 12, 2006
Licensed Content Volume	6
Licensed Content Issue	11
Type of Use	reuse in a dissertation / thesis
Requestor type	academic/educational
Format	print and electronic
Portion	figures/tables/illustrations
Number of figures/tables /illustrations	1
High-res required	no
Figures	Figure 2 from the article
Author of this NPG article	no
Your reference number	
Title of your thesis / dissertation	Basigin-2-mediated activation of ERK1/2 in human glioblastoma cells
Expected completion date	Jul 2017
Estimated size (number of pages)	95

APPENDIX B

License to use Figures 1 and 2 from “The microenvironment of the tumour-host interface” by Liotta and Kohn received from Nature Publishing Group.

License Number	4143290388065
License date	Jul 06, 2017
Licensed Content Publisher	Nature Publishing Group
Licensed Content Publication	Nature
Licensed Content Title	The microenvironment of the tumour-host interface
Licensed Content Author	Lance A. Liotta and Elise C. Kohn
Licensed Content Date	May 17, 2001
Licensed Content Volume	411
Licensed Content Issue	6835
Type of Use	reuse in a dissertation / thesis
Requestor type	academic/educational
Format	print and electronic
Portion	figures/tables/illustrations
Number of figures/tables /illustrations	2
Figures	Figure 1 and Figure 2 from the article.
Author of this NPG article	no
Your reference number	
Title of your thesis / dissertation	Basigin-2-mediated activation of ERK1/2 in human glioblastoma cells
Expected completion date	Jul 2017
Estimated size (number of pages)	95